CORROSION FATIGUE OF INCONEL 625 EXPLOSION BONDED TO NICKEL ALLOY STEEL

John Carmine Scalzo

CORROSION FATIGUE OF INCONEL 625 EXPLOSION BONDED TO NICKEL ALLOY STEEL

BY

JOHN CARMINE SCALZO
LIEUTENANT, UNITED STATES NAVY
B.S., UNITED STATES NAVAL ACADEMY
(1967)

SUBMITTED IN PARTIAL FULFILLMENT
OF THE REQUIREMENTS FOR THE DEGREE OF
OCEAN ENGINEER
AND THE DEGREE OF
MASTER OF SCIENCE IN

CORROSION FATIGUE OF INCONEL 625 EXPLOSION BONDED TO NICKEL ALLOY STEEL

John Carmine Scalzo

Submitted in partial fulfillment of the requirements for the Degree of Ocean Engineer and the Degree of Master of Science in Naval Architecture and Marine Engineering to the Department of Ocean Engineering.

ABSTRACT

The explosion bonding of Inconel 625 to nickel alloy steel will not reduce the fatigue or corrosion fatigue strengths of either metal, judging from metallurgical analysis and studies of crack initiation and growth. Scale model tests and economic studies of marine applications, such as propeller shaft sleeves, should therefore be carried out. Metallurgical investigation before and after bonding and stress relieving showed no adverse effects at the interface except for a slight increase in sensitivity of the steel to etching. The fatigue and corrosion fatigue lives of the Inconel, tested at 1800 cpm, were not reduced during bonding and the interface did not appear to be a source of weakness.

The corrosion fatigue strength of the bonded steel at the interface was not reduced by bonding. Crack propagation rates of cracks growing from the Inconel into the steel were near those of the unbonded metals. Cracks were observed to turn away from the hardened metal at the interface. Intentional defects placed at the interface reduced the mechanical strength but at the same time tended to act as crack stoppers.

Thesis Supervisor: Frank A. McClintock
Title: Professor of Mechanical Engineering

ACKNOWLEDGEMENTS

I would like to thank Mr. Robert Colton, who I worked with last summer at the Army Materials and Mechanics Research Center. His professional advice and assistance were invaluable to me in formulating this research program. I would also like to thank the United States Navy for sponsoring this thesis, especially Mr. Joseph Crisci of the Naval Ship Research and Development Center for his encouragement and direction in pursuing this research, as well as in obtaining the funds for its completion. I wish to thank those people at the Boston Naval Shipyard; especially Mr. Thomas Foley, head of Shop 31; Mr. Ralph Petraglia, in charge of ultrasonic testing; and Mr. Marty Graham, head of the Materials Testing Laboratory; for all the work they performed in support of this research. My appreciation goes to Mr. Henry Otto at the Denver Research Institute for performing the bonding of the plates, and to Mr. William Henry of MIT for his technical assistance, especially in the design of the salt water cell. I would like to thank Huntington Alloys Division of the International Nickel Company for also providing material and technical assistance. My special appreciation goes to Professor Frank A. McClintock, my thesis supervisor, for his professional guidance and encouragement throughout

this project. And finally, I reserve my warmest and deepest gratitude to my wonderful wife Jackie, who not only expertly typed this manuscript and assisted in the preparation of the figures, but also provided me with much needed encouragement and inspiration throughout this past year.

TABLE OF CONTENTS

I. INTRODUCTION

The U.S. Navy has been investigating the possibility of cladding propulsion shafting with Inconel alloy 625 to replace the current copper-nickel shrink fit sleeves. The present sleeves are used to protect the shafting from the damaging effects of sea water at critical areas external to the hull. The shaft arrangement, shown in Figure 1, shows the copper-nickel sleeves at the stern tube shaft seal, strut bearing journal, and adjacent to the propeller.

Several problems can exist on the present shaft sleeves. The first is due to the cyclic bending stresses produced by the overhanging propeller. These stresses, combined with the corrosive action of the sea water, can result in corrosion fatigue damage to the sleeve. Another problem is at the shaft seal where a potential difference exists between the hull and seal components with the shaft being anodic to the hull. This can result in general corrosion of the shaft sleeve. A third problem is fretting corrosion at the interface between the shaft and sleeve. This is caused by slight relative slip between the metals which occurs due to their different elastic moduli.

A search for a more corrosion resistant material and a better application technique was conducted by the Navy. Inconel 625 was considered as a possible replacement for

copper-nickel (Miller and Belt, 1970). Various application methods are now being considered in order to find one which best retains the excellent properties of the Inconel. Initially a weld overlay technique was evaluated. Results showed that the corrosion fatigue strength of the weld metal was only half that of the wrought Inconel base plate (Williams, 1967). Explosive cladding is considered as another application method, one in which the properties of the clad metal would be more like that of the base plate than the weld metal. The advantages of cladding with Inconel 625 include improved corrosion fatigue resistance, improved resistance to the general corrosion at the shaft seal, and the elimination of fretting corrosion. These improvements would lead to extended periods between overhauls and improved reliability and maintainability of propulsion shafting.

This research was intended to help evaluate Inconel 625 as a propeller shaft sleeve replacement by determining the fatigue and corrosion fatigue properties of the explosion bonded material. Cracks initiating in the Inconel were examined and the fatigue life determined for the unbonded and bonded metal in both air and salt water. Crack propagation was investigated as a crack grew, as it would in service, from the Inconel into the steel. The effect of an unbonded area at the interface and crack growth from a machined notch were also examined. End effects, where the

interface would be exposed at the end of a sleeve, were not specifically studied. The use of current fiberglass protective coatings and the feathering of the bond edges could be used to reduce the effects of salt water and the stress concentration at the interface.

II. MATERIALS & PROCESSING

A. MATERIAL PROPERTIES

The steel base plate was a forged nickel-molybdenum steel used by the Navy for propeller shafting. The specification is MIL-S-23284 (SHIPS) Class 2. The actual piece obtained was a 16-inch long section of shaft manufactured by National Forge Company (Heat #4-0262), taken from a 14-inch diameter shaft made for the Navy. The chemical composition and mechanical properties reported by the manufacturer are shown in Table I (Pike, 1972).

Inconel is a registered trademark of the International Nickel Company, Inc. Alloy 625 is a nickel-chromium alloy used for its high strength, excellent fabricability, and outstanding corrosion resistance in fresh and salt water. The strength of the alloy is derived from the strengthening effect of molybdenum and columbium on its nickel-chromium matrix. In salt water the alloy is said to be free from pitting, crevice corrosion, and stress corrosion cracking (The International Nickel Company [INCO], 1970). The Inconel* was obtained in the form of 1/8-inch and 3/16-inch cold-rolled sheet. The chemical composition and mechanical

*Hereafter, "Inconel" will refer to Inconel 625.

properties as reported by the supplier for the 1/8-inch sheet (Heat #NX79B2AK) are shown in Table II (Alcan Aluminum Company, 1972). The 3/16-inch piece was a 6-inch by 12-inch sample provided by the International Nickel Company.

To verify the reported mechanical properties hardness tests were performed on the steel and the Inconel when received. Tests across the diameter of the steel shaft showed there was no noticeable reduction in hardness at the center of the shaft. These tests and hardness tests taken on each 1/2-inch plate cut from the shaft showed the steel to have a hardness of 94 R_B. According to Lyman (1961) this corresponds approximately to a tensile strength of 99,000 psi which verifies the 98,250 psi reported by the manufacturer. The hardness of the 1/8-inch Inconel sheet as received was 95 R_B. Tests performed on a 1/8-inch sample piece after solution annealing at 2100°F for half an hour showed a reduction in hardness to 88 R_B. The hardness of the 3/16-inch sample piece as-received was 94 R_B.

Tensile tests were performed on the 1/8-inch Inconel sheet before and after solution annealing. These tests were done to verify the strength reported by the manufacturer and to determine the amount of increased ductility obtained during the solution annealing. The results of these tests, shown in Table III, agree with that reported by the manufacturer and show the expected increase in ductility due to solution annealing.

B. PROCESSING

1. Prior to Bonding

The shaft section was cut into 1/2-inch thick disks and squared off into 10-inch-square plates. Each plate was Blanchard ground in preparation for the Inconel cladding. The cladding of the Inconel on the face of the disk represents a situation different from the actual application. In practice the Inconel would be clad around the outer diameter of the shaft. It was recognized that the mechanical properties of the steel would vary somewhat across the face and differ from the properties at the perimeter of the shaft due to the thickness and direction of the shaft forging. However, this method of application was chosen since it provided the most practical method for testing purposes. The possibility of using a rolled steel plate was considered in order to get uniform properties underneath the cladding but it was decided that using the actual shaft steel would provide more useful information than using a steel with different chemical composition.

The Inconel was obtained in the form of cold-rolled sheet because of its availability and suitability to the bonding configuration. The 1/8-inch sheet used for the bonding was cut into twelve 10-inch-square plates. It should be noted that the mechanical properties, particularly the fatigue strength, vary significantly for the different

forms of the material. Table IV gives an example of this variation (INCO 1970; Williams, 1967).

Previous work in bonding Inconel 625 to A516 steel for pressure vessels done by du Pont indicated that better bond properties are obtained when the Inconel is bonded in the solution annealed condition (Hix, 1972). It was found that cracks may occur at the interface when the bonding is done in the harder mill annealed condition. Solution annealing softens the Inconel and allows for more plastic deformation at the bond. This annealing was performed on the 1/8-inch sheet prior to bonding by heating at 2100°F for 1/2-hour and furnace cooling. This produced an oxide layer on the surface of the plates which had to be removed by pickling. Development of a suitable pickling process for the twelve plates, lettered A through L, is described in Table V.

2. Bonding

Explosion bonding is a solid phase welding process. The pieces to be joined are impacted together usually by the detonation of an explosive on the surface of one metal. The explosive force is used to create the high impact velocity required for welding. A typical bonding configuration for flat plates is shown in Figure 2. This shows the flyer plate, base plate, explosive, and angular standoff between the plates.

When the explosive ignites it forces the plates together at a high velocity. At the junction between the plates a jetting action occurs which removes thin metal surface layers from both metals. This brings freshly exposed metal surfaces into contact under high pressure which causes the actual bonding. There are three basic requirements for welding to occur: 1) an impact velocity high enough to produce plastic flow, 2) the formation of the jet at the point of contact, and 3) an oblique angle of impact (Carpenter and Wittman, 1970).

There is little or no melting or intermixing of the metals. This is important because it means no intermetallic compounds are formed which may weaken the weld. The fact that no mixing takes place allows explosive welding to be used on a variety of dissimilar metals. An interesting property of the weld is a characteristic waviness at the bond line as shown in Figure 3. There are many theories regarding the exact method of formation of this but most ascribe to the action of the jet as it moves over the surface.*

The bond itself is a metallurgical bond resulting in a highly cold-worked area at the bond line. The cold-working results in both metals becoming harder and stronger

---

* For a detailed description of the explosion bonding process see Carpenter and Wittman, 1970; Crossland and Williams, 1968; and Lucas, Williams, and Crossland, 1970.

at the interface. Tensile tests on bonded metals usually result in failure in the weaker of the two metals rather than at the bond. Numerous mechanical tests have been performed on different configurations of bonded metals and the results show that the bond strength is usually as good as the weaker of the two metals being joined (Banerjee and Crossland, 1971; De Maris and Pocalyko, 1966; Carpenter and Wittman, 1970; Savidge, 1971).

The explosion bonding of the Inconel to steel for this research was performed at Denver Research Institute. The twelve plates were welded at a T standoff using 40% Red Cross Extra dynamite. Plate F was welded using a loading of 11 grams/inch^2, plate C was welded using 12 grams.inch^2, and all others were welded with 11.5 grams/inch^2 loading. Two plates, A and K, were purposely bonded with a non-bond line down the center to simulate a defect during testing. These non-bond zones, which varied in width from 1/2 to 1 inch, were obtained by using a non-bonding agent which was paint containing alumina.

3. After Bonding

The cold-working at the bond zone can cause extensive strain hardening at the interface. This results in a large hardness gradient from the interface extending into the metals. A microhardness profile typical of explosion bonded metals usually shows a large discontinuity at the bond

interface. Stress relief annealing has been recommended for bringing the hardnesses of the materials closer together (Savidge, 1971). This post-bond annealing should return some ductility to the bond zone without significantly reducing the strength.

In order to determine a satisfactory stress relief, samples were taken from one plate and sample stress reliefs performed at 1000°F for 2, 4, 6, and 8 hours. The aim was to achieve a moderate reduction in hardness while not initiating grain growth or diffusion. Superficial Rockwell hardness readings were taken across the bond before and after each anneal and compared to each other. The results, shown in Table VI, show that the 4 hour stress relief appeared to give the desired moderate decrease in hardness in the Inconel. On this basis it was decided to give all the bonded plates a 4 hour stress relief.* After pressing each plate to remove a 1/10-inch bowing caused by the bonding, each was stress relieved and cut into specimens for testing.

---

* It was realized at this point that in order to accurately determine the effect of the different holding times, microhardness tests and metallography would have to be conducted on each sample. However lack of time precluded this being done. Microhardness tests were later conducted on another plate before and after stress relieving for 4 hours to better show the effect of the stress relief.

II. TESTING AND RESULTS

A. PRELIMINARY TESTS

1. Microhardness Tests

Microhardness tests were performed on samples from one plate before and after stress relieving. These tests give some indication of the amount of strain hardening which occurs at the bond interface and the effect of the 4 hour stress relief on the hardness at the interface. Hardness profiles across the as-bonded interface can vary considerably, but the general result is that the hardness of both materials is increased, due to both shock-hardening and localized interfacial work-hardening due to severe plastic flow (Crossland and Williams, 1968).

The microhardness results, shown in Figures 4 and 5, show the rapid increase in hardness at the interface due to the bonding process.* These results are consistent with the superficial hardness tests previously taken, but also show a much higher hardness closer to the interface. The stress relieved sample shows that the stress relieving had a much greater effect on the steel than on the Inconel.

---

* These results are average values for 4 traverses taken at each interface area.

This result did not appear in the superficial tests because the wider spacing of the superficial tests did not give a good indication of the hardness gradient within 0.1 mm of the interface. After stress relieving, the hardness of the steel is greatly reduced, in fact, the hardness actually decreases as the interface is approached closer than 0.05 mm, as shown in Figure 4. This behavior has been previously noted (Savidge, 1971; Crossland and Williams, 1968) and, as reported by Crossland and Williams, may be caused by partial recrystallization in the highly cold-worked steel. The work done by Savidge on the bonding of Inconel 600 to ASTM A 302 steel shows hardness profiles very similar to these results both before and after stress relieving.

A result not found in the literature is that, before annealing, higher hardness values appear at the crest of a wave than at the trough of a wave at the same distance from the interface.* This was found in both the Inconel and the steel. Figure 6 demonstrates this by showing average hardness values along two different lines of traverse. The wave height of the interface is 0.1 mm. At a distance of about 2 wave heights away from a trough in Inconel and 1 wave height away from a trough in steel the hardness is

---

* For 4 traverses the average hardness difference at 0.03 mm from the interface was 544 Vickers in the Inconel and 285 Vickers in the steel.

uniform along the weld.

2. Ultrasonic Testing

After the 1/8-inch Inconel was explosively bonded on to the steel plates, each plate was ultrasonically tested to determine the presence of defects or unbonded areas. This was done at the Boston Naval Shipyard Ultrasonic Laboratory using a Branson Sonoray 50C Ultrasonic Flaw Detector. This detector is used in the field to test silver brazing bonds in pipe joints and the babbit-to-shell bonds in bearings. It is the type of instrument which would be used in the field to test the bond on a shaft. The plates are manually scanned using a hand held transducer at 2.25 M hertz and pulse rate of 300cps. The sensitivity of the flaw detection is 1/64-inch for a flat bottom hole.

The results of this testing showed that, except for an area about 1/2-inch to 1 inch wide along the edges of the plates, no defects were detected. In the flat plate bonding configuration it is normal to have this unbonding at the edges due to the manner in which the explosive is detonated. In a cylindrical bonding configuration an unbonded area may occur at the line of detonation at one end of the sleeve. This unbonded region can be removed by machining, thereby not presenting a problem in service. The detector also clearly showed the unbonded area in the plates with the intentional non-bond zone down the center.

3. Metallography

Metallographic samples were taken from the Inconel in the following conditions: 1) as-received, 2) solution annealed, 3) as-bonded, and 4) bonded and stress relief annealed. Steel samples were taken in the as-bonded and stress relief annealed conditions. Sections were taken parallel to the longitudinal transverse plane, rolling plane, and short transverse plane. The Inconel was etched electrolytically using a 20% Nital solution and the steel was etched using 2% Nital.*

The effect of the solution annealing on the Inconel before bonding is shown in Figures 7 and 8. The grain size is increased from ASTM No. 7.5 to ASTM No. 3. This result is consistent with the observed increased ductility and reduction in tensile strength as previously shown in Table III. Also evident are numerous inclusions, along which grain boundaries tend to be aligned. These inclusions are reported to be mostly carbides, rich in nickel, columbium and molybdenum. In both figures the roll direction is evident in the longitudinal orientation of the inclusions.

Figure 9 shows the microstructure of the Inconel in the rolling plane in the (a) as-bonded and (b) stress

---

* The metallography was performed at the Materials Testing Laboratory of Boston Naval Shipyard.

relieved conditions. The photomicrographs are taken at a distance of approximately 1/8-inch from the interface. The microstructure again shows a large amount of inclusions, especially at the grain boundaries. Apparent in the Inconel are twinning planes, which are evidence of plastic deformation in crystals where layers of atoms slide bringing the deformed part of the crystal into a mirror-image orientation relative to the undeformed part of the crystal. The figures show that there is no apparent difference in the microstructures before and after stress relieving at 1/8-inch from the interface. The grain size is about the same in each (ASTM No. 3) and there is no change in the amount or location of the inclusions.

Figures 10 through 12 show the microstructure of the Inconel in the short transverse plane at each step in the processing. Figures 10(b) and 11(b) again show the increased grain size and concentration of inclusions at grain boundaries resulting from solution annealing. Figure 12(a) shows the microstructure of the as-bonded Inconel at the bond interface. The grain size has remained the same as before bonding with the grain boundaries showing more clearly at a distance of 2 wave heights (0.2 mm) from the interface. The highly cold-worked area at the interface does not show any grain structure, but concentrations of inclusions are apparent. The stress relieved sample in Figure 12(b) shows essentially the same

Inconel grain size as the as-bonded sample, and the inclusions are still visible at the interface. These results correspond to the microhardness results which showed that the stress relief had very little effect on the Inconel except within 0.01 mm of the interface.

Unetched samples of the bond interface are shown in Figures 13(a) and 14(a). These are longitudinal views which clearly show the wavy characteristic of the interface. An interesting observation is that the inclusions have agglomerated on one side of the wave crest at the interface. The bonding direction is not known for certain in these views but upon comparison to a schematic representation of the wave formation, shown in Figure 15, which was postulated by Bahrani, and reported by Carpenter and Wittman (1970), it is assumed that the bonding direction was downward in each case resulting in the inclusions appearing at the forward side of the waves.

Figures 13(b) and 14(b) show the steel microstructure before and after stress relieving. Both figures show that at the interface the grains lose their clarity, apparently realigning along the wave front. This may be due to an actual reduction in grain size or grain distortion, both of which are consistent with the microhardness results showing a large amount of cold-working at the interface. Comparing the grain structure before and after stress relieving, it is seen that there is no apparent change in

grain structure, other than at the interface. At the interface the etchant has caused the steel to appear darker than before stress relieving. The darkening effect is greater in the steel crests and extends further from the interface at the crests than at the troughs. The explanation of this is not certain. Correlating these results to the microhardness tests before and after stress relieving it can be seen that the darkening had greater effect where the steel was hardened the most, i.e. at the crests. This may draw upon the conclusions that the stress relieving may have caused partial recrystallization at the more highly cold-worked areas. The expected recrystallization temperature for the steel of this composition is about 1300°F. However, the highly cold-worked region of the bond zone may begin to recrystallize at the 1000°F annealing temperature. Another possible explanation is that diffusion of some metals may have occurred at the interface. This however, is unlikely due to the short annealing time of 4 hours at 1000°F. A preliminary investigation across the interface with an energy dispersive x-ray analyzer (EDAX) did not indicate that any diffusion had occurred. A more likely explanation of this darkening effect is that the stress relieving causes an interaction between diffusion or precipitation and the dislocation structure at the highly cold-worked interface. This can produce a change in microstructure

resulting in the increased sensitivity to the etchant.

B. FATIGUE TESTING

Fatigue tests were performed at 1800 cpm on unbonded Inconel and steel and on the bonded composite to determine what effect the explosion bonding process had on the fatigue and corrosion fatigue resistance of the metals. The Inconel is the material of prime interest in these tests since it would be clad on the external surface of the steel where fatigue cracks would most likely start. The detailed procedure of the various fatigue tests, including specimen design and sample stress calculations, is presented in the Appendix. The following is a brief description of the tests, including the results and discussion.

1. Unbonded Inconel

The unbonded Inconel sheet was tested in cantilever bending. Specimens were taken from both the 3/16-inch sample and the 1/8-inch sheet. All specimens were cut so that the fatigue crack propagated perpendicular to the rolling direction. This orientation provides maximum resistance to crack growth. Stresses on the Inconel in service would be steady torsion and alternating bending as compared to the reversed bending applied during testing. The criterion for failure was crack propagation until specimen deflection exceeded the testing machine maximum deflection of 0.35 inches. This produced cracks extending

from half-way to completely through the specimen.

Ten 3/16-inch and seven 1/8-inch specimens were tested in air. The results, shown in Figure 16, show that the fatigue strength at 10^7 cycles was about 47,000 psi. This compares favorably with the fatigue strength of 38,000 psi at 10^8 cycles reported by the manufacturer (INCO, 1970).

Six 1/8-inch specimens were tested in a 3% NaCl solution with a pH between 5 and 7. The aerated salt water was circulated in a closed system around the specimens at an approximate velocity of 10 feet per second. The results, shown in Figure 16, show that at 10^7 cycles the fatigue strength in salt water was reduced to 40,000 psi. At 47,000 psi, the salt water reduced the fatigue life by a factor of ten. The two curves begin converging at higher stress levels apparently indicating that the salt water had less affect on fatigue life in tests which lasted less than 3×10^5 cycles, or about 3 hours. Corrosion fatigue tests conducted at a lower frequency, which would allow a longer time for the same number of cycles, should show a greater reduction in strength below 10^5 cycles. Uhlig (1971) has reported that the lower the frequency of stress application, the more effectively does the corrosive environment shorten fatigue life. This means that the time of exposure to the corrosive environment, or amount of corrosive attack, as well as the number of cycles to

failure, is an important parameter to consider when predicting corrosion fatigue life.

Uhlig also states that corrosion fatigue damage is greater than the sum of damage by corrosion and fatigue acting separately. Each factor contributes to overall damage but the resistance of a metal to corrosion fatigue is associated more nearly with its inherent corrosion resistance than with its high mechanical strength. The high corrosion resistance of Inconel 625 makes it attractive as a cladding material to protect steel in a salt water environment. The corrosion fatigue life of Inconel at stress levels above 40,000 psi is actually greater than the fatigue life of the steel in air, as shown in Figure 16.

2. Bonded Inconel to Steel

The bonded specimens were tested in reversed bending with the directions of rolling and bonding of the Inconel parallel to the specimen length. This produced crack growth perpendicular to both the rolling and bonding direction. In service, this corresponds to bonding the Inconel in the roll direction, parallel to the shaft length. The specimen was designed so the fatigue cracks initiated in the Inconel and propagated into the steel, since this is the way cracks would most likely grow in service. The criterion for failure was again crack propagation until specimen deflection exceeded the maximum allowed machine

deflection, here an amplitude of 0.40 inches. The cracks propagated from one-third to half-way through the specimen thickness before the test terminated.

Six bonded specimens were tested in air and the results are shown in Figure 17. When compared with the unbonded Inconel the results show that the fatigue life of the Inconel was not reduced due to the explosion bonding process. All cracks initiated at the outer surface of the Inconel, and the bond interface did not appear to be a source of weakness in crack initiation or propagation.

Previous fatigue testing of explosion bonded metals has provided a variety of results. De Maris and Pocalyko (1966) conducted bending fatigue tests on Inconel 600 clad to ASTM A-302-B FbQ steel, and type 304-L stainless steel, Timet 35-A titanium, and "Hastelloy" alloy C all separately clad to ASTM A-212-B FbQ backing steel. The Inconel 600 clad to steel specimens were tested so that the bond zone was in the plane of maximum flexural shear. The results showed that the fatigue properties of the steel were not adversely affected and those of the Inconel were about the same as the unclad Inconel. Fatigue tests on the other metal combinations were conducted with the bond zone as close as practical to the maximum alternating stress plane. These results showed a reduction in fatigue strength of the backing steels. In all of these tests the interface was not a source of weakness in fatigue failure. Savidge

(1971) performed flat plate bending tests on Inconel 600 and Inconel 606 bonded to ASTM A-302 steel with the bond zone at the plane of maximum flexural shear. The results showed no difference between the explosion bonded 600 to steel and a weld overlay on the steel. Banerjee and Crossland (1971) performed tensile fatigue tests on stainless steel clad to steel, and brass clad to steel, and in both cases they found the fatigue strength of the composite was as good as, or a little better than, the stronger of the two materials. However, they noted that cracks did initiate at the interface.

The variation of results can be partially attributed to different bonding techniques and different metal combinations. The use of optimum bonding parameters is necessary to avoid any melting at the interface producing weak intermetallic compounds, and to avoid any bond defects. The types of metals being joined can also affect the resulting metallurgical bond properties.

Figure 17 shows the points for the bonded Inconel, compared to the curves for the unbonded Inconel and those obtained by Williams (1967) on hot-rolled, annealed Inconel plate and welded Inconel to steel. The unwelded plate has a fatigue strength of 58,000 psi at 10^7 cycles, but the weld metal has a fatigue strength of only 37,000 psi. Additionally, no endurance limit is observed for the

weld metal, even at stresses as low as 31,000 psi. The joining of the metals by explosion bonding results in higher fatigue strengths than the conventional welding technique.

The decreased fatigue resistance of the Inconel weld metal results from the heat input during welding which caused iron diffusion into the Inconel and a change in microstructure. Properly bonded Inconel will have little or no melting at the interface and no metal mixing should occur. The original metallurgical properties will be affected only a small distance on either side of the interface. Microhardness tests on these plates showed that the hardness increased significantly only within 0.2 mm on either side of the interface. The microstructure also did not seem to be affected beyond this distance. The metallurgical properties of the base metal are retained, unlike during conventional welding, and the fatigue strength of the Inconel is not reduced.

Seven bonded specimens were tested in 3% NaCl solution in a system similar to that used to test the unbonded specimens. The specimens were coated to protect the steel and the Inconel-steel interface from the salt water. This was done to determine the effect of the bonding on the Inconel only. The exposed Inconel surface was 1/16-inch from the interface.

The results, shown in Figure 18, show that the corrosion fatigue life of the bonded Inconel is about the same as the unbonded Inconel. Cracks in properly coated specimens started at the Inconel surface and propagated into the steel with no evidence of weakness at the interface. Once the crack entered the steel, rapid corrosion of the steel occurred with corrosion products being carried out of the crack to the surface. The appearance of the Inconel was the same as during the unbonded tests in salt water.

Comparing these results to those obtained for a weld overlay of Inconel 625 (Williams, 1967), Figure 18, shows that again a longer life is obtained with an explosion bonded clad than with a weld overlay. This is once again attributed to the retention of these base metal properties during explosion bonding.

3. Fatigue Crack Propagation

Fatigue crack propagation rates were measured in cracks growing from the Inconel, through the interface, and into the steel. Specimens like those shown in Figure A3 were tested at 1800 cpm with a notch machined in the Inconel to act as a crack starter. The notch geometry is shown in Figure 19. The purpose of these tests was to compare crack growth rates in the bonded materials with existing data on unbonded Inconel and steel.

Linear-elastic fracture mechanics defines a stress

intensity factor to describe the stress and displacement fields around a growing crack.* This is practically useful for correlating crack growth rates under test and service conditions. According to fracture mechanics fatigue crack growth rate depends on the stress intensity factor at the crack tip.

The stress intensity factor K_I for this specimen geometry and loading can be estimated from the stress concentration factor (scf) at the tip of the notch. The stress concentration factor was determined, according to Neuber (1968), to be approximately 4.5 for a notch radius of $\underline{a}$ = .005 inches. For a crack separation (Mode I) mode of relative motion between the faces of the crack, the stress intensity factor can be calculated from the nominal applied net stress (σ_n) using the following equation (see for example McClintock, 1971):

$$K_I = \lim_{a \to o} (scf)\, \sigma_n \frac{\sqrt{a\pi}}{2}$$

Since these equations apply only in an elastic stress region, it is important to estimate the size of the plastic zone at the crack tip. Numerical solutions by Levy et al. (1971), and reported by McClintock (1971) show that the

---

* For a detailed explanation of fracture mechanics for corrosion fatigue see McClintock (1971).

maximum extent of the plastic zone for Mode I can be approximated, given the yield strength Y, by the equation:

$$r_I = \frac{.5\left(K_I\right)^2}{\pi\left(Y\right)}$$

For these testing conditions the plastic zone size was 0.006 inches.

The dependence of crack growth rate on stress intensity factor has been investigated by Paris (1964) and correlations established between crack growth rate per cycle ($d\ell/dn$) and stress intensity factor range (ΔK), where ΔK is defined as $K_{Imax} - K_{Imin}$ for each cycle. Using the above equation for K_I, ΔK for the tests performed was determined to approximately 14,000 psi $\sqrt{\text{in.}}$. Using the method reported by Paris and Sih (1965), ΔK was determined to be approximately 12,000 psi $\sqrt{\text{in.}}$. To determine $d\ell/dn$, an average growth rate was calculated based on total crack length and an estimated number of cycles of crack propagation. This estimate was based on observation of specimen compliance during testing and the total number of cycles of testing.

Two specimens were tested in air and two in salt water. The results of the tests, shown in Figure 20, show a higher crack growth rate in the salt water than in air, as is expected. As also shown in Figure 20, the present crack growth rates are in general close to those of Long

(1972) for Inconel 625 and this type of steel at the lower range of stress intensity values. More specifically, when Long's data are extrapolated to this lower stress intensity value it is seen that the crack growth rates in the explosion bonded Inconel and steel are higher than those of the base metals and within the band of data for the weld metal.*

4. Other Fatigue Tests

Unbonded steel specimens were tested in air and salt water to determine approximate fatigue life curves. The results, shown in Figure 16, were in agreement with those reported by the Navy for this type of steel. It is again noted that the curves tend to converge at shorter life, this time at about 10^5 cycles, or one hour.

Two bonded specimens were tested in salt water with the interface exposed. The results were that the fatigue crack initiated in the steel at the interface. The lives of the specimens were slightly above those found for the unbonded steel specimens, but could be considered within the acceptable scatter band. This indicates that the bonding process did not reduce the corrosion fatigue life

---

* It is noted that the present tests were performed on cold-rolled sheet which has a shorter fatigue life than the hot-rolled plate tested by Long.

of the steel at the interface.

Specimens with a 1/2-inch x 1/4-inch intentional defect at the test section were also tested in air and salt water. Two specimens were tested in salt water, with the interface coated, at 50,000 and 56,000 psi. The results were that the corrosion fatigue life was reduced by about a factor of 4. The specimen tested in air at 56.000 psi had a reduction in fatigue life of about 8. This indicates that the defect acted more to affect the mechanical fatigue strength of the Inconel than the corrosion fatigue strength. In fact, as shown in Figure 29(b) in Fractography, the specimen tested in air had crack initiation at the interface, rather than at the surface, probably due to the rougher surface finish there.

Three specimens with a defect were tested with a machined notch in the Inconel. The cracks initiated at the notch tip below 10^4 cycles and immediately propagated through the Inconel. Once the crack reached the defect at the interface, it stopped. The specimen then essentially behaved like an unbonded section of steel with no crack initiating in the steel since the stress was below the endurance limit. These results indicate that the implanted defect acted as a crack stopper at the interface.

C. FRACTOGRAPHY

The fractographs presented provide information regard-

ing sites of crack initiation and direction of propagation and the presence of general corrosion in the tested specimens. They are intended to aid in the interpretation of the experimental results and provide incite into possible service failures. Figures 21(a) and (b) show the fracture surface for unbonded Inconel specimens in air and salt water respectively. The fracture surface of specimens in both air and salt water appeared as a gray, silky, fibrous ductile fracture. There was no evidence of general corrosion or pitting in any specimen in salt water.

Bonded specimens tested in air and salt water are shown in Figures 22 and 23. Figure 22(a) shows a profile of the crack as it grew in air from the Inconel into the steel. The crack appears jagged in the Inconel and becomes straighter as it propagated in the steel. Figure 22(b) shows the fracture surface with the crack apparently initiating in the left hand corner near the interface.

A bonded specimen tested in salt water is shown in Figure 23. The general corrosion of the steel is clearly seen. The steel was attacked by the salt water from the inside as the crack grew into the steel. The wavy interface can be seen in (b), and the crack tip, showing salt and corrosion deposits, is shown in (c). The fracture surface, (d), shows evidence that the crack initiated in the upper left surface of the Inconel.

Fracture surfaces of cracks which initiated in the steel in air and salt water are shown in Figures 24(a) and (b) respectively. Both cracks appeared to have initiated along the top flat surface. The corroded steel surface is evident in the salt water specimen.

Cracks which started near the interface are shown in Figures 25 and 26. Figure 25 shows the cracking of a bonded specimen in salt water with the interface exposed. The two sides of the specimen, shown in (a) and (b), show that general corrosion took place more on one side than on the other. In (b), the initiation of secondary cracks is evident; in (c), a close up of the largest secondary crack, starting at the interface, is shown. The fracture surface, (d), shows that the crack initiated in the steel at the left side of the interface.

A specimen tested in salt water which developed a defect in the coating is shown in Figure 26. Salt water attacked the steel underneath the coating causing the crack to initiate in the steel. The deep pit into the steel is seen in (b) to occur just below the interface in the steel. Visible above the pit are the wave crests in the steel. The fracture surface, (d), clearly shows evidence the crack started near the interface.

The fatigue crack appearance of specimens which contained the intentional defects is shown in Figures 27

through 29. The surface of a specimen tested in salt water, Figures 27(a) and (b), shows a major and a secondary crack, both initiating in the Inconel. As the crack reached the interface it approached the unbonded zone and stopped. Another crack then initiated in the steel at one end of the unbond. Figure 28(a) shows the Inconel fracture surface with the crack apparently initiating in the upper left corner. The steel fracture surface is shown in (b) with the crack appearing to have several nucleation sites, typical of a high stress level.

A similar crack appearance for a salt water specimen is shown in Figure 29(a). The fracture surface of a specimen tested in air with a defect is shown in Figure 29(b). In this specimen the crack in Inconel appears to have initiated at the interface. The stress in this plane would only be 80% of that at the outer surface, but the outer surface was polished compared to the area at the unbond which was rough. This is one apparent reason for the crack initiating at the interface. In the salt water specimens the corrosion at the surface increases the tendency for the crack to initiate at the surface rather than at the interface. The steel fracture surface appears to have many crack nucleation sites, similar to the specimen tested in salt water.

The fatigue cracks in the crack propagation specimens tested in air are shown in Figures 30(a) and (b). These

fractographs clearly show a turning crack path as it approaches the interface. This turning crack pattern was typical of the majority of all specimens tested, both fatigue life specimens and crack growth rate specimens. The crack in Figure 30(a) is particularly interesting since it turns away from an Inconel crest, grows toward a trough, and when it reaches the interface at a steel crest it runs along the interface and grows into the steel from a trough. Similar behavior was observed on 50% of the crack propagation specimen cracks at the surface. This crack growth pattern underscores the results of the hardness profile obtained at the interface (Figure 6), which indicated more hardening at a crest than at a trough for each metal. The cracks in the other specimens followed a more random path after the initial sharp angle turn. The fatigue cracks appear to be turning away from the more highly strain hardened metal at the interface. Figure 30 (b) also shows the crack turning almost 90 degrees as it approaches the interface. It is noted that the crack begins its sharp turn at a distance of about one wave height (0.1mm) from a trough along the interface. This was the case for most of the sharp angled cracks. The hardness profiles showed that at this distance the hardness of the metal began its sharp increase. (See Figures 4, 5, and 6)

Figures 31(a) and (b) show the crack pattern in salt water. Both again show the crack turning sharply. In (a) corrosion products are seen at the tip of the notch in the Inconel. Figure 31(b) shows corrosion products at the interface where the crack penetrated the steel. Closer observation showed that these products resulted from corrosion of the steel.

IV. RECOMMENDATIONS AND CONCLUSIONS

The purpose of this work was to evaluate the fatigue and corrosion fatigue properties of Inconel 625 explosion bonded to nickel alloy steel. This evaluation was based on analysis of the change in microstructure during bonding, the effect of bonding on the fatigue life, and the observation of crack growth through the bond interface. The results show that explosion bonding is an attractive application method. Further study, including a scale model of a shaft and an economic analysis, is warranted.

Microhardness tests before and after bonding showed that the bonding process resulted in an increase in hardness from 200-300 Vickers to above 900 Vickers within 0.03mm of the interface in both metals. A characteristic wave formation was produced at the interface with a wave height of 0.1mm. More hardening occurred at the crests of the waves in each metal than at the troughs, with a uniform hardness profile obtained about two wave heights from the interface at a trough. In the Inconel, the only noticeable change in microstructure caused by the bonding was an agglomeration of inclusions along one side of each wave crest. Stress relieving at 1000°F for 4 hours reduced the hardness at 0.03 mm from the interface to 400-500 Vickers

in the steel, but only to about 800 Vickers in the Inconel. The stress relieving caused a higher sensitivity to the etchant of the hardened steel at the interface while apparently not affecting the microstructure of the Inconel.

The fatigue strength of the cold-rolled Inconel sheet at 10^7 cycles was found to be 47,000 psi in air and 40,000 psi in salt water. Salt water reduced the fatigue life by a factor of ten at 47,000 psi. The explosion bonding process did not reduce the fatigue or corrosion fatigue life, tested at 1800 cpm. The interface, with an in-plane stress of 80% of the maximum flexural stress, was not a source of weakness. The fatigue life in both air and salt water proved to be longer than previous reported results for a weld overlay of Inconel on steel.

When the interface was exposed to the salt water fatigue environment, cracks tended to start in the steel at the interface, but at a life not less than that for the unbonded steel. This shows that the bonding and stress relieving process did not reduce the corrosion fatigue strength of the steel at the interface.

Crack propagation rates were measured for cracks growing from the Inconel, through the interface, and into the steel. The crack growth rate was found to be slightly higher than those reported for the unbonded base metals, and within the band of those reported for a weld overlay of

Inconel.* The crack growth rate in salt water was found to be 50% higher than that in air.

Observation of the crack growth through the interface revealed that cracks tended to turn sharply when approaching the hardened interface, apparently to avoid the more highly hardened metal at a crest compared to that at a trough. Cracks were found not to propagate along the interface, even when made to grow out of a defect at the bond. Once a crack entered a defect from the Inconel it stopped and re-initiated in the steel at the end of the defect.

In summary, it appears from a fatigue and corrosion fatigue point of view, that explosion bonding is a desirable method of joining Inconel 625 to steel. The microstructure is not degraded during bonding and the good corrosion resistant properties are retained. The fatigue life is maintained in air and salt water and cracks are even seen to turn from the bond interface.

---

* The present tests were performed on cold-rolled sheet which, as reported by the manufacturer, has a lower fatigue life than the hot-rolled plate for which the previous crack growth rates were reported.

V. BIBLIOGRAPHY

1. Alcan Aluminum Company, Metal Goods Division, Material Test Results, September 13, 1972.

2. Banerjee, S. K. and Crossland, B., "Mechanical Properties of Explosively Cladded Plates," Metal Construction, July 1971.

3. Carpenter, Steve H. and Wittman, Robert H., "The Theory and Application of Explosion Welding," Denver Research Institute, 1970.

4. Crossland, B. and Williams, J. D. "Explosive Welding," Metallurgical Reviews, Transactions AIME, Volume 212, June 1968, pp. 79-100.

5. DeMaris, J. L. and Pocalyko, A., "Mechanical Properties of Detaclad Explosion Bonded Clad Metal Composites," ASTME Engineering Conference Paper AD 66-113, 1966.

6. Hix, Hugh duPont Company, Personal Communication July 13, 1972.

7. Lucas, W., Williams, J. D. and Crossland, B. "Some Metallurgical Observations on Explosive Welding," Proceedings of the Second International Conference of the Center for High Energy Forming, Denver, Colorado, 1969.

8. Lyman, Taylor, Metals Handbook, 8th Edition, Volume I, American Society for Metals, Metals Park, Ohio, 1961, p. 1234.

9. McClintock, Frank A., "Fracture Mechanics for Corrosion Fatigue," International Conference on Corrosion Fatigue, University of Connecticut, Storrs, Connecticut, June 14-18, 1971.

10. McClintock, Frank A. and Argon, Ali, Mechanical Behavior of Materials, Addison-Wesley Publishing Company, Reading, Massachusetts, 1966, p. 592.

11. Miller, Boyce E. and Belt, J. R., "Imposed Voltage Corrosion of Materials for Submarine Shaft Seals," Naval Ship Research and Development Center Report 3207, April 1970.

12. Neuber, Dr.-Ing. H., Kerbspannungslehre, Second Edition, Springer-Verlag, Berlin, 1968, Figure 148.

13. Paris, P. C.,"The Fracture Mechanics Approach to Fatigue." Proceedings 19th Sagamore Army Materials Research Conference, Syracuse, New York, 1964.

14. Paris, Paul C. and Sih, George C.,"Stress Analysis of Cracks," Fracture Toughness Testing and its Applications, ASTM-STP-381, American Society for Testing and Materials, Chicago, Illinois, 1965, p. 41.

15. Pike, R. J., Certification of Test Results, National Forge Company, September 26, 1972.

16. Savidge, R.,"Mechanical Properties of Explosion Clad Bonds of High Nickel Alloys on Low Alloy Steel and the Effect of Explosion Cladding on Fracture Properties of Steel," Proceedings of the Third International Conference of the Center for High Energy Forming, Vail, Colorado, July 12-16, 1971.

17. The International Nickel Company, Inc., "Heating and Pickling the Huntington Alloys," 1968.

18. The International Nickel Company, Inc., "Inconel Alloy 625," 1970.

19. Uhlig, Herbert H., Corrosion and Corrosion Control, John Wiley and Sons, Inc., 1971, pp. 147-156.

20. Williams, W. L. (by direction), "Fatigue Properties of Plain and Welded Inconel 625 Alloy," Naval Ship Research and Development Center Report MEL 454/67, December 22, 1967.

OTHER GENERAL REFERENCES NOT SPECIFICALLY REFERRED TO IN THE TEXT

1. Burke, John J., Reed, Norman L. and Weiss, Volker, editors, Fatigue an Interdisciplinary Approach, Proceedings of the 10th Sagamore Army Materials Research Conference, Syracuse University Press, 1964.

2. Committee E-9 on Fatigue, Manual on Fatigue Testing, American Society for Testing and Materials, Special Technical Publication No. 91, 1949

3. Fink, F. W. and Boyd, W. K., The Corrosion of Metals in Marine Environments, Defense Metals Information Center, Battelle Memorial Institute, Columbus, Ohio, Bayer and Company, Inc., 1970.

4. Forrest, P. G., Fatigue of Metals, Pergamon Press and Addison-Wesley Publishing Company, Inc. 1962.

5. Harbage, Alfred B., "Fatigue Study of a Monel Inlaid Shaft Exposed to Seawater." Naval Ship Research and Development Center Report 7-353, April 1970.

6. Kallas, D. H. (by direction), "Inconel 625 Weld Overlays for Cladding Propulsion Shafting," Naval Ship Research and Development Center letter, Annapolis Laboratory, 2823:CAZ, 10310, May 22,1972.

7. Snapp, R. B., "Submarine Propeller Shaft-Seal Corrosion," U.S. Navy Marine Engineering Laboratory Report 512/66, March, 1967.

8. Schwab, R. C. and Czyryca, E. J., "Effects of Notches and Salt Water Corrosion on the Flexural Behavior of High-Strength Structural Alloys," Effects of Environment and Complex Load History on Fatigue Life, ASTM-STP-462, American Society for Testing and Materials, 1970.

9. Tetelman, A. S. and McEvily, A. J. Jr., Fracture of Structural Materials, John Wiley and Sons, Inc. New York, 1967.

10. Wolfe, R. J. (by direction), "Inconel 625 Weld Overlays," Naval Ship Research and Development Center Report 28-50, December 13, 1971.

APPENDIX

DETAILED FATIGUE TESTING PROCEDURE

A. UNBONDED INCONEL

1. Specimen Design

The unbonded Inconel sheet was tested in cantilever bending at 1800 cpm on a Sonntag model SF-2U fatigue testing machine. All tests were conducted at room temperature. The Inconel was tested as-received in the cold-rolled, mill annealed condition. The specimen design is shown in Figure A1, with t equal to 0.1875 inches for the ten specimens from the sample piece, and 0.125 inches for the seven other specimens. The rolling direction was longitudinal for all specimens. The surface finish was tested with a Cleveland Roughness Meter and the average roughnesses, measured longitudinally, were as follows:

Location	Average Roughness (μ in.)
Flat top surface	5
Machined notch	20
Machined sides	60

2. Stress Calculation

A sample stress calculation using the maximum applied

load of 25 pounds is presented.

$$\sigma_A = \frac{My}{I} = \frac{(F_A)\ (L)\ (h/2)}{bh^3/12}$$

F_A = applied load = 25 lb

L = moment arm = 3 in.

h = test section height = 0.08 in.

b = test section width = 0.75 in.

σ_A = applied stress = 93,750 psi

3. Salt Water Environment

The salt water tests were conducted in a 3% NaCl solution. The salt water was circulated around the specimen at an approximate velocity of 10 feet per second. Sufficient air was circulated to provide an aerated mixture. The pH was monitored by using indicator paper and was in the neutral range of 5-7 for all tests. A schematic of the laboratory set-up is shown in Figure A2.

B. BONDED INCONEL TO STEEL

1. Specimen Design

The bonded specimens were cut from the bonded plates with the specimen length parallel to the bonding direction and Inconel roll direction. Material within 3/4-inch of the border of the plates was not used because of the possibility of a poor bond in this area. All tests were con-

ducted at room temperature with the specimens in the stress relief annealed condition.

The design of the specimen was dictated by the desire to initiate cracks on the Inconel surface when testing in both air and salt water. Since the fatigue strength of the Inconel was higher than that of the steel, a trapezoidal cross section was used to place the neutral axis closer to the steel surface than the Inconel. This, along with the use of a mean load, produced the desired stress distribution. The specimen design is shown in Figure A3. After machining, the specimens were longitudinally hand polished down to 320 grit paper. The surface finish was tested with a Cleveland Roughness Meter and the average roughnesses, measured longitudinally, were as follows:

Location	Average Roughness (μ in.)
Inconel top surface	5
Steel bottom surface	10
Tapered machined sides	150

2. Stress Calculations

A sample stress calculation for the test section using an applied load of 200 pounds is presented.

$$\sigma_{A_{INCO}} = \frac{(M)\ (y_{INCO})}{(I_t)} = \frac{(F_A/2)\ (L)\ (y_{INCO})}{(I_t)}$$

F_A = applied load = 200 lb

L = moment arm = 6 in.

y_{INCO} = distance of Inconel surface to neutral axis

$$y_{INCO} = h\left[1 - \frac{2a+b}{3(a+b)}\right]$$

I_t = moment of inertia of trapezoidal cross section

$$I_t = \frac{h^3(b^2 + 4ab + a^2)}{36(a + b)}$$

for a = 0.25 in.

b = 0.50 in.

h = 0.50 in.

y_{INCO} = 0.28 in.

I_t = 0.0038 in.

$\sigma_{A_{INCO}}$ = 44,210 psi

$$\sigma_{A_{STEEL}} = \frac{(M)(y_{STEEL})}{(I_t)}$$

$y_{STEEL} = h - y_{INCO}$ = 0.22 in.

$\sigma_{A_{STEEL}}$ = 34,736 psi

A mean load was applied as necessary to produce the required stress distribution. The combined static and alternating loads were extrapolated to zero mean load to obtain the equivalent stress at zero mean load. This was done according to McClintock and Argon (1966) and the stress

pattern used is shown in Figure A4. A sample calculation is presented to demonstrate the procedure.

1. An applied alternating load of 200 lb results in an alternating stress on the outer Inconel surface of 44,210 psi, and on the outer steel surface of 34,736 psi.
2. An applied mean load of 50 lb results in a tensile mean stress on the outer Inconel surface of 11,052 psi, and a compressive mean stress on the outer steel surface of 8,684 psi.
3. The resulting stress on the Inconel (point A in Figure A4) is equivalent to about 48,00 psi (point B) at zero mean load.
4. The resulting stress on the steel (point C) is equivalent to about 33,000 psi (point D) at zero mean load.

3. Salt Water Environment

The salt water tests were conducted in a 3% NaCl solution with the salt water circulating as previously described for the unbonded tests. Since the corrosion fatigue strength of the steel is only about one-fourth that of the Inconel a coating had to be placed on the steel to allow crack initiation in the Inconel. A "stop-off lacquer", which is a paint-like coating, was applied

on the bottom and sides of the test section, leaving only the top Inconel flat surface exposed to salt water.* Despite these precautions two specimens failed by cracking in the steel. The stress level was high enough to obtain data for the Inconel, showing the life was at least as long as the time for failure in the steel, as shown in Figure 18. Three other tests were terminated at 10^6 or more cycles before any failure with similar data points obtained.

---

* The Inconel-steel interface was purposely protected to determine the effect of bonding on the Inconel only. Other specimens were tested with the interface exposed, and the results are noted elsewhere.

TABLE I.

Chemical Composition and Mechanical Properties of Shaft Steel.

CHEMICAL COMPOSITION	
Element	Wt. %
C	0.22
Ni	3.02
Mn	0.34
Mo	0.34
Cr	0.21
Si	0.19
V	0.07
S	0.007
P	0.006

MECHANICAL PROPERTIES	
UTS (psi)	98,250
YS (psi)	77,500
Elongation (%)	24.5
Reduction in area (%)	65.4
Charpy Impact (ft-lb @ 30°F)	31.5

TABLE II.

Chemical Composition and Mechanical Properties of Inconel 625.

CHEMICAL COMPOSITION	
Element	Wt. %
Ni	60.61
Cr	21.94
Mo	8.78
Fe	4.22
Cb + Ta	3.57
Ti	0.32
Si	0.24
Al	0.18
Mn	0.07
C	0.04
P	0.005
S	0.004

MECHANICAL PROPERTIES	
UTS (psi)	136,000
YS (psi)	73,500
Elongation (%)	49
Hardness (R_B)	98
Elastic Modulus (psi)	30×10^6
ASTM Grain Size	7.5

TABLE III.

Tensile Tests on Inconel Before and After Solution Annealing

	AS RECEIVED	SOLUTION ANNEALED
	(SAMPLE #1)	
UTS (psi)	134,200	124,500
YS (psi)	-	60,100
Elongation (%)	43.8	47.7
	(SAMPLE #2)	
UTS (psi)	134,200	121,500
YS (psi)	70,400	52,800
Elongation (%)	46.9	56.3

TABLE IV.

Mechanical Properties of Different Production Forms of Inconel 625

FORM AND CONDITION	UTS(ksi)	YS(ksi)	FAT. STR.(ksi)
Bar (Hot-rolled)			
Annealed	120-150	60-95	95 @ 10^7cycles
Solution-Treated	105-130	42-60	70 @ 10^7cycles
Plate (Hot-rolled)	120-150	60-95	55 @ 10^7cycles*
Sheet (Cold-rolled)			
Annealed	120-150	60-90	38 @ 10^8cycles

---

* Obtained from Williams (1967), all other data from INCO (1970).

TABLE V.

Description of Pickling
Process for the Twelve Inconel Plates

Plates B, H, I, J, K, and L*

1. Soaking for 30 to 40 minutes in the following solution:

   1000 cc water

   296 cc nitric acid

   50 cc hydroflouric acid

2. Soaking for 5 to 6 hours in the following solution:

   60% water

   40% sulfuric acid

All plates (A through L)**

1. Fine sandblast
2. Soaking for 30 to 40 minutes in:

   1000 cc water

   296 cc nitric acid

   50 cc hydroflouric acid

All plates were then heated at 375°F for three hours to remove any hydrogen.

---

* Pickled according to manufacturers recommended procedure. (INCO, 1968).

** The recommended procedure did not completely remove the oxide scale. Due to lack of available facilities, notably a fused salt bath, the follow-up recommended procedure could not be completed. Therefore, the sandblast was performed, which did remove the oxide scale.

TABLE VI.

Hardness Test Results Before and After Sample Stress Relieving*

Two Hour Stress Relief

Distance From Interface (in.)	As Bonded Hardness Rockwell 30N		After Stress Relief Hardness Rockwell 30N
1/8	45		44
3/32	45	Inconel	46
1/16	47		47
1/32	48		51
1/32	44	Interface	42
1/16	42		42
3/32	41	Steel	42
1/8	41		42

Four Hour Stress Relief

1/8	44		45
3/32	49	Inconel	46
1/16	50		48
1/32	59		54
1/32	45	Interface	45
1/16	45		41
3/32	42	Steel	41
1/8	41		41

* All stress relieving done at 1000°F followed by an air cool.

TABLE VI. (cont'd)

Six Hour Stress Relief

Distance from Interface (in.)	As Bonded Hardness Rockwell 30N		After Stress Relief Hardness Rockwell 30N
1/8	52		48
3/32	52	Inconel	52
1/16	53		51
1/32	56		53
		Interface	
1/32	44		43
1/16	44		42
3/32	43	Steel	41
1/8	44		41

Eight Hour Stress Relief

1/8	52		53
3/32	52	Inconel	54
1/16	53		55
1/32	54		58
		Interface	
1/32	47		44
1/16	43		44
3/32	44	Steel	44
1/8	45		45

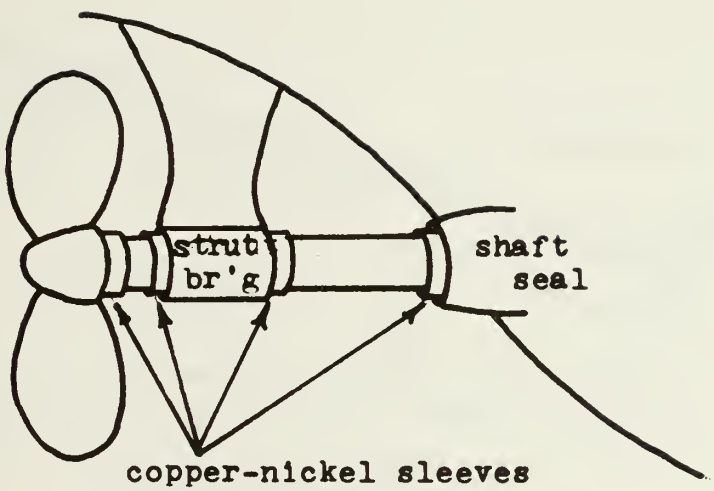

Figure 1 - Propeller Shaft Arrangement External to the Hull.

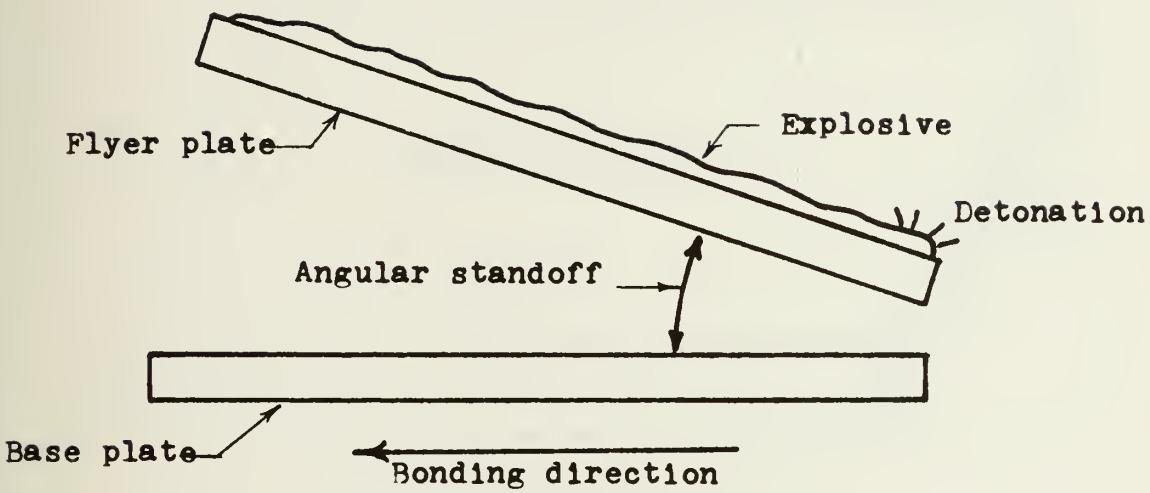

Figure 2 - Typical Bonding Configuration for Flat Plate

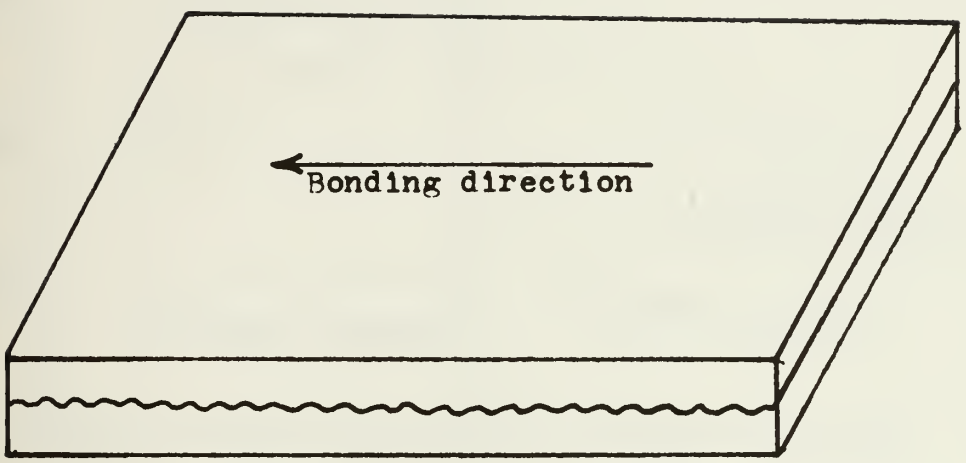

Figure 3 - View of Explosion Bonded Plate Showing Characteristic Waviness at Interface.

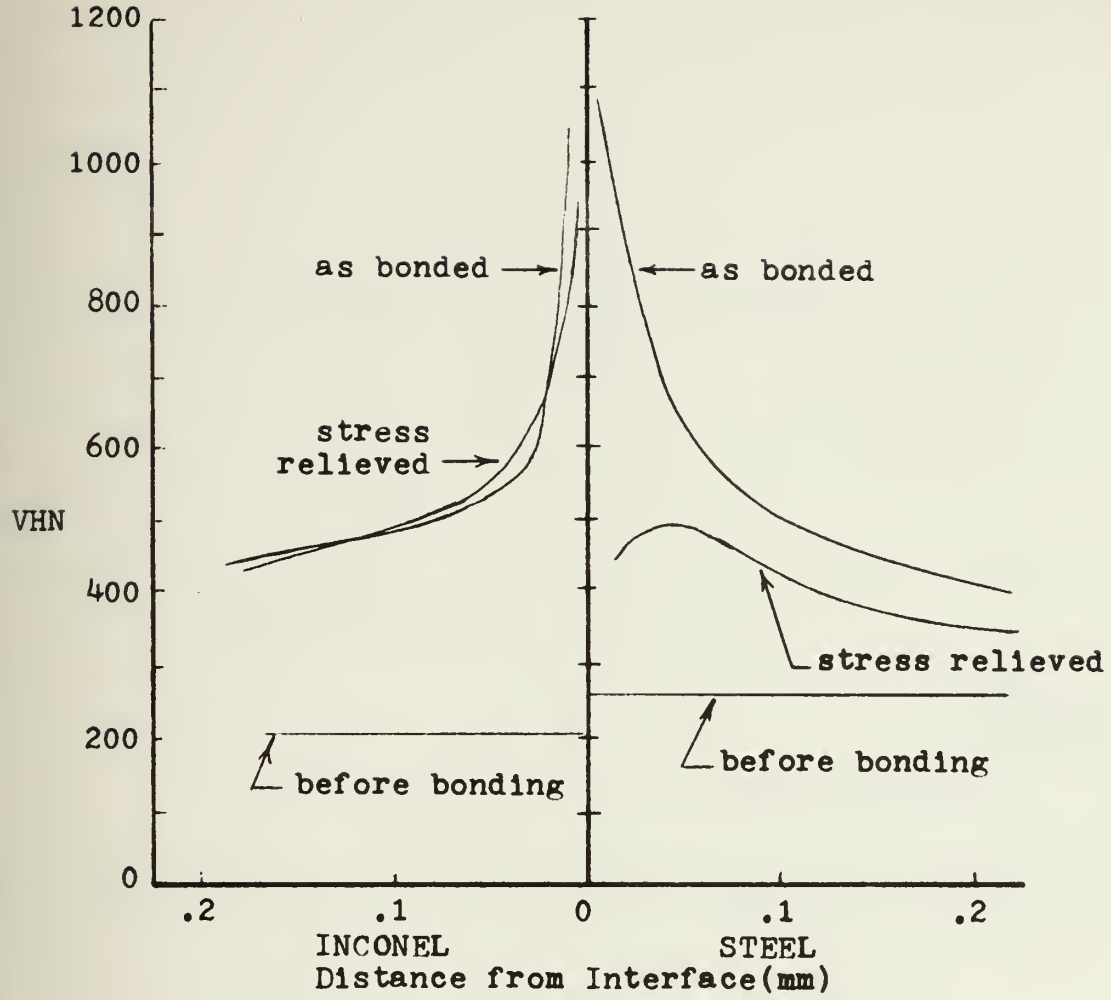

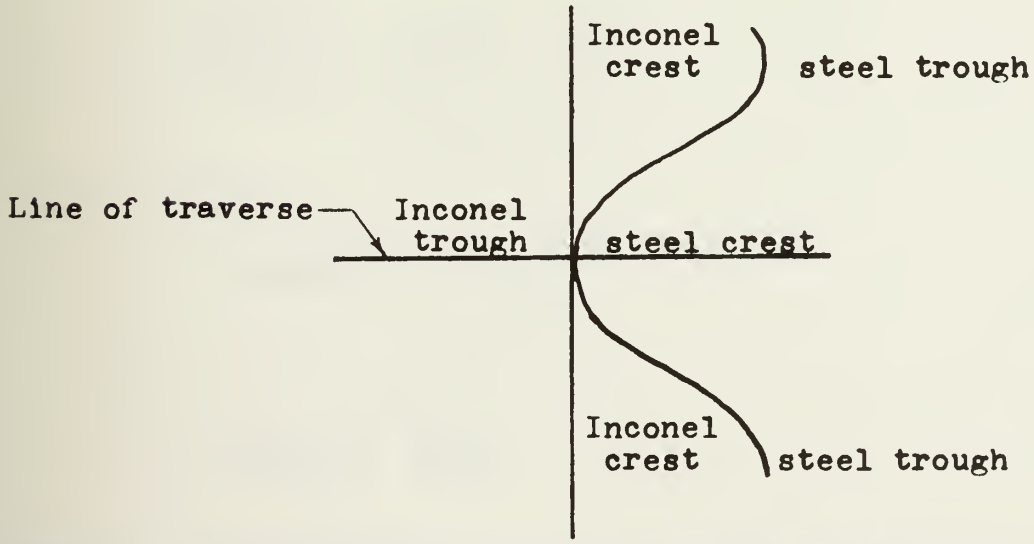

Figure 4 - Microhardness Traverse Across the Explosion Bonded Interface at a Steel Crest.

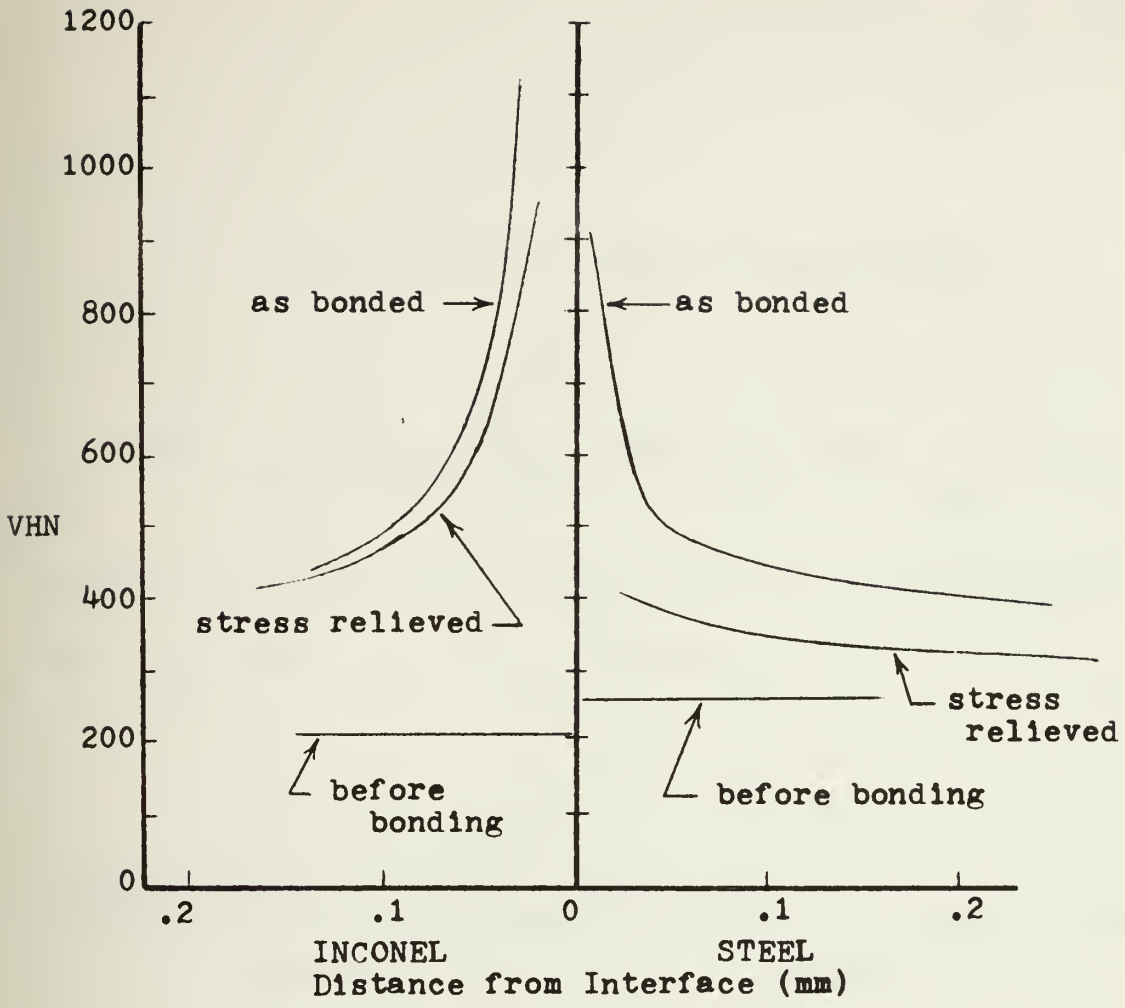

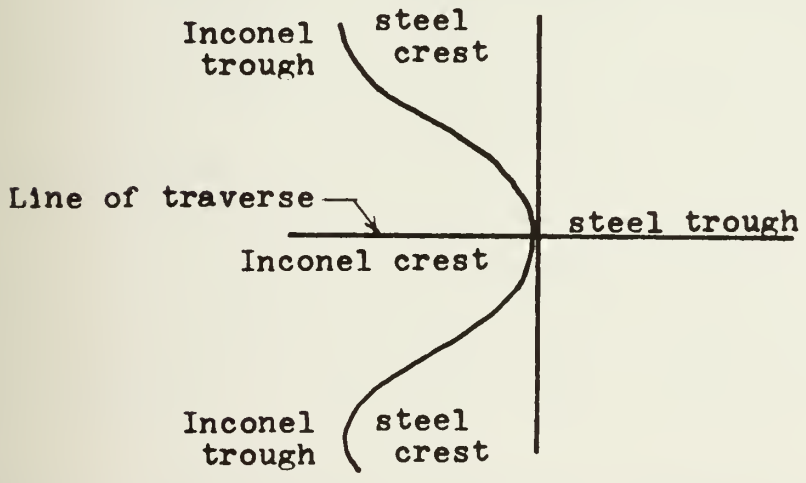

Figure 5 - Microhardness Traverse Across the Explosion Bonded Interface at a Steel Trough.

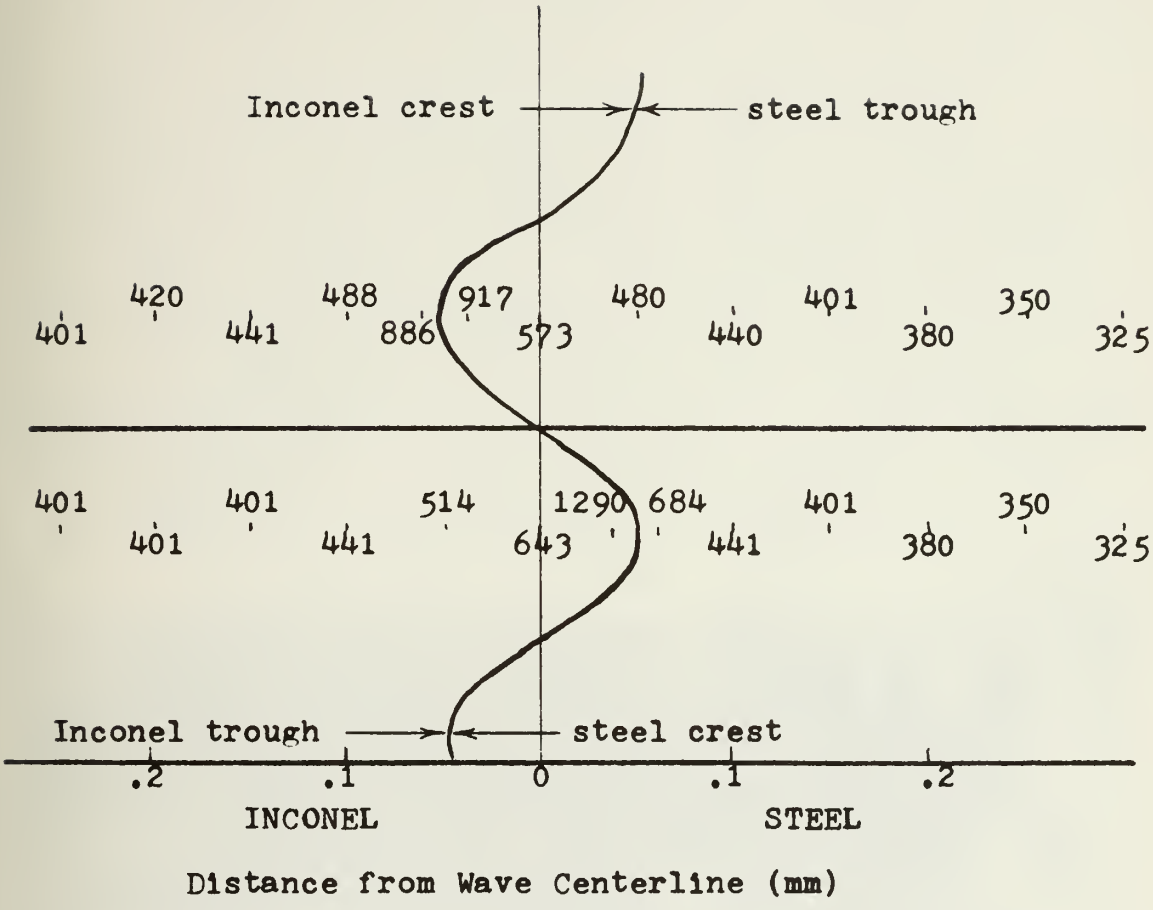

Figure 6 - Microhardness Results, Vickers (As-Bonded)

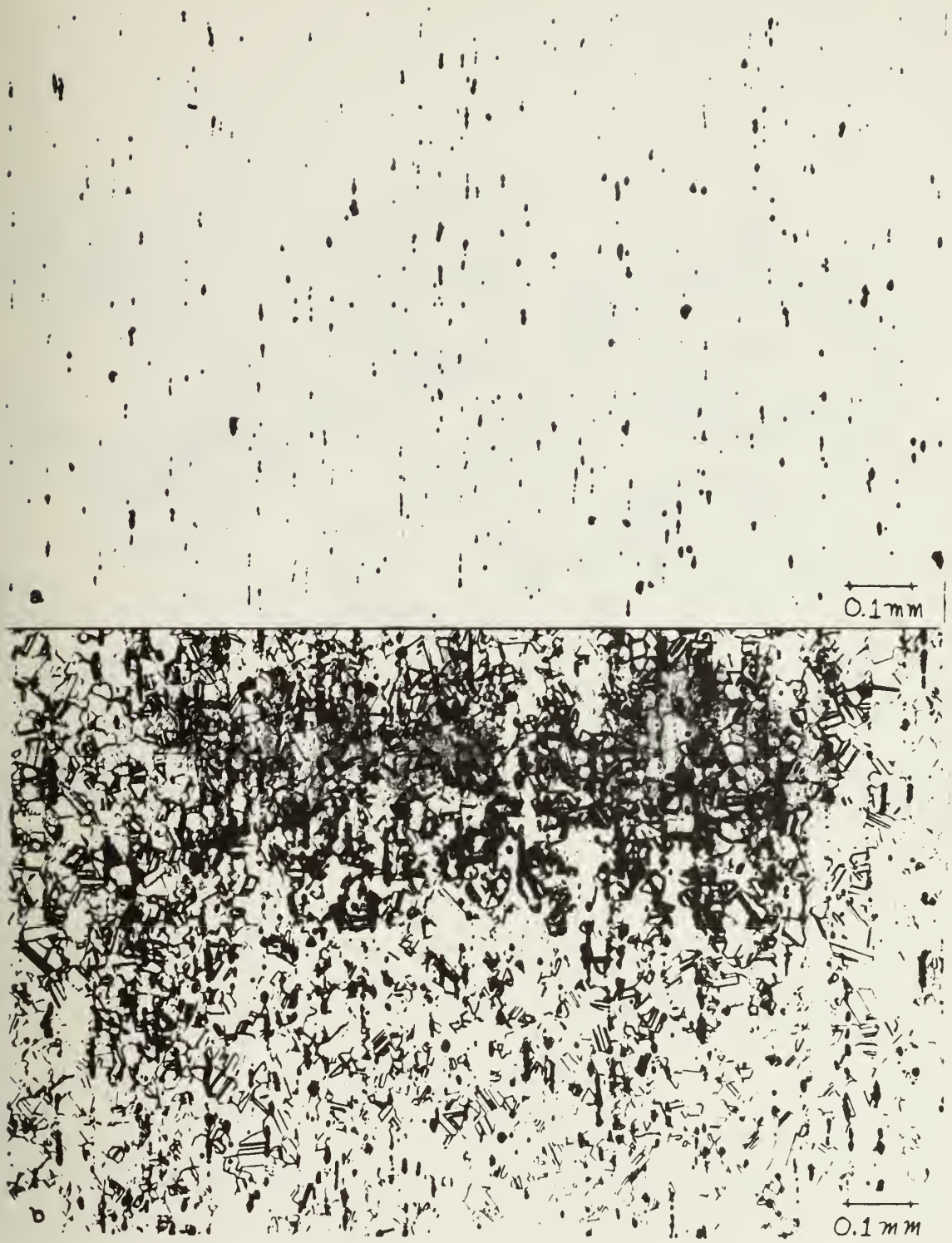

Figure 7 - Longitudinal Inconel Section As-Received
(a) Unetched and (b) Etched

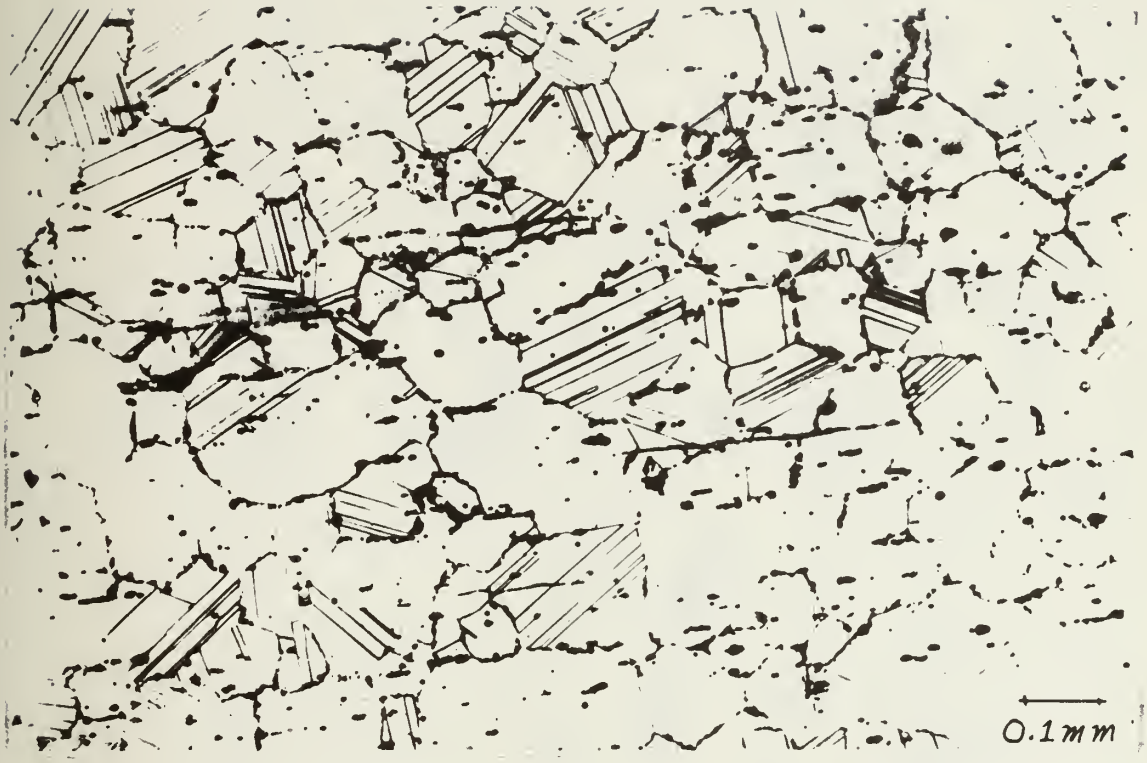

Figure 8 - Longitudinal Inconel Section after Solution Annealing

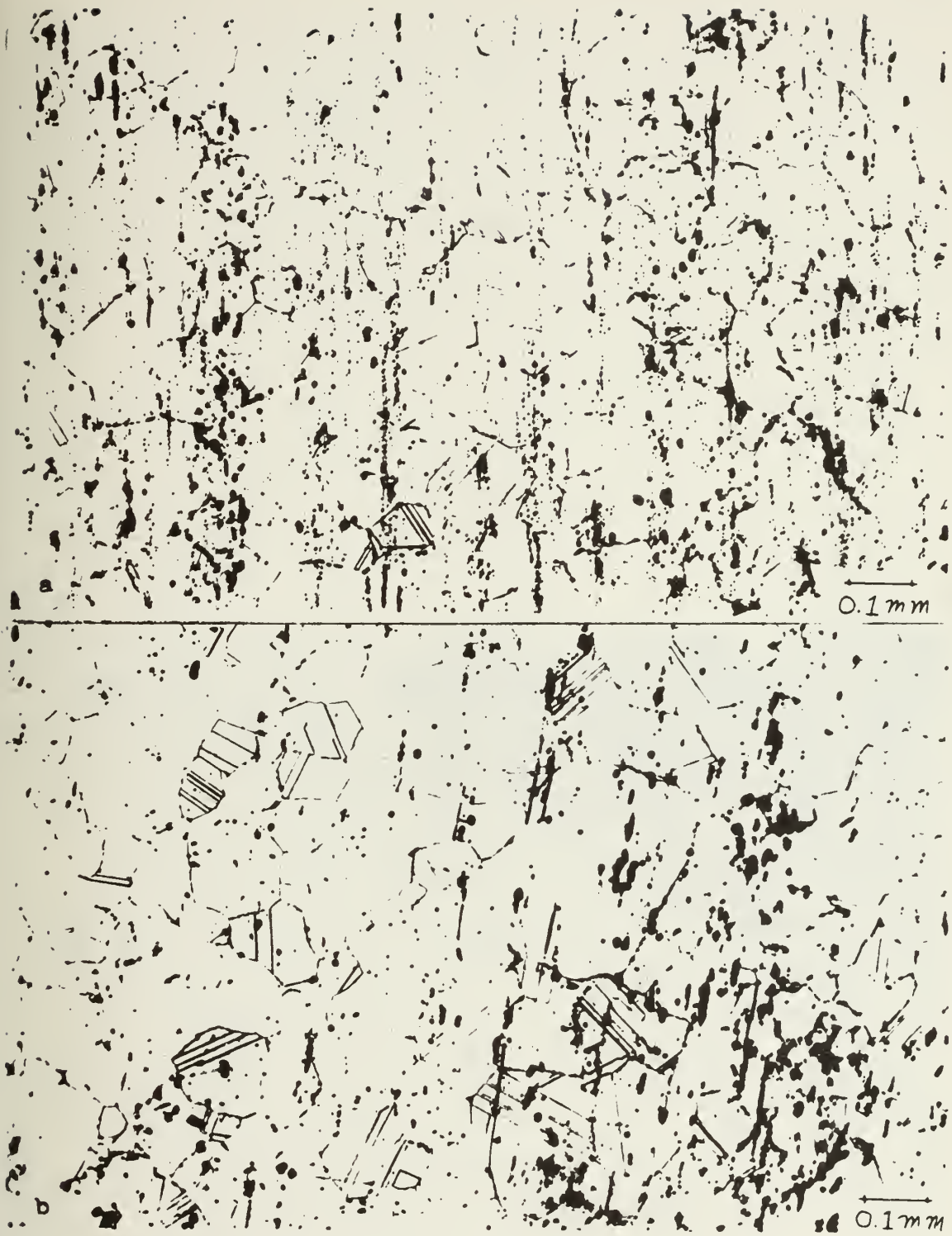

Figure 9 - Rolling Plane Inconel Section (a) As-Bonded and (b) Stress Relieved

Figure 10 - Short Transverse Inconel Section As-Received
(a) Unetched and (b) Etched

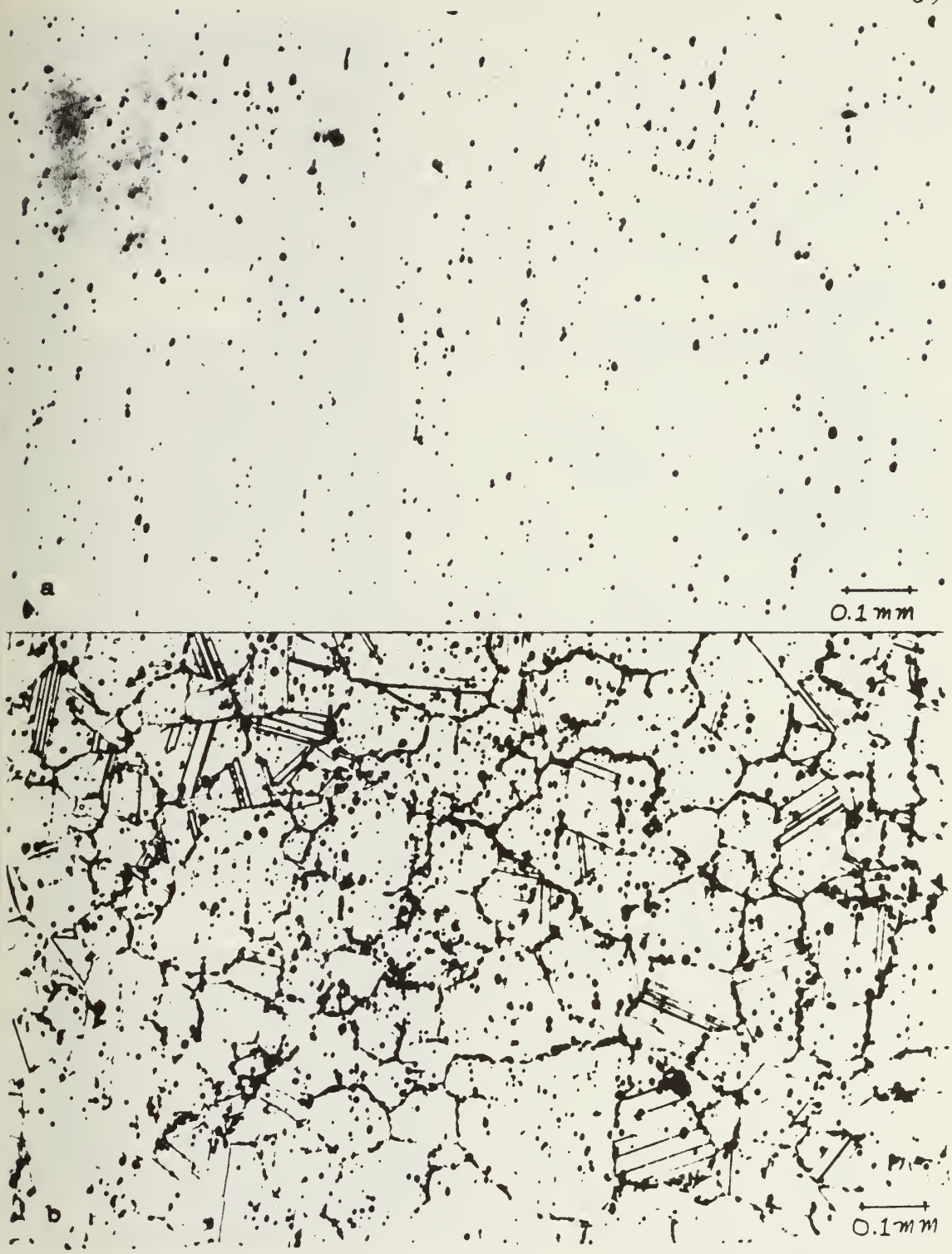

Figure 11 - Short Transverse Inconel Section After Solution Annealing (a) Unetched and (b) Etched

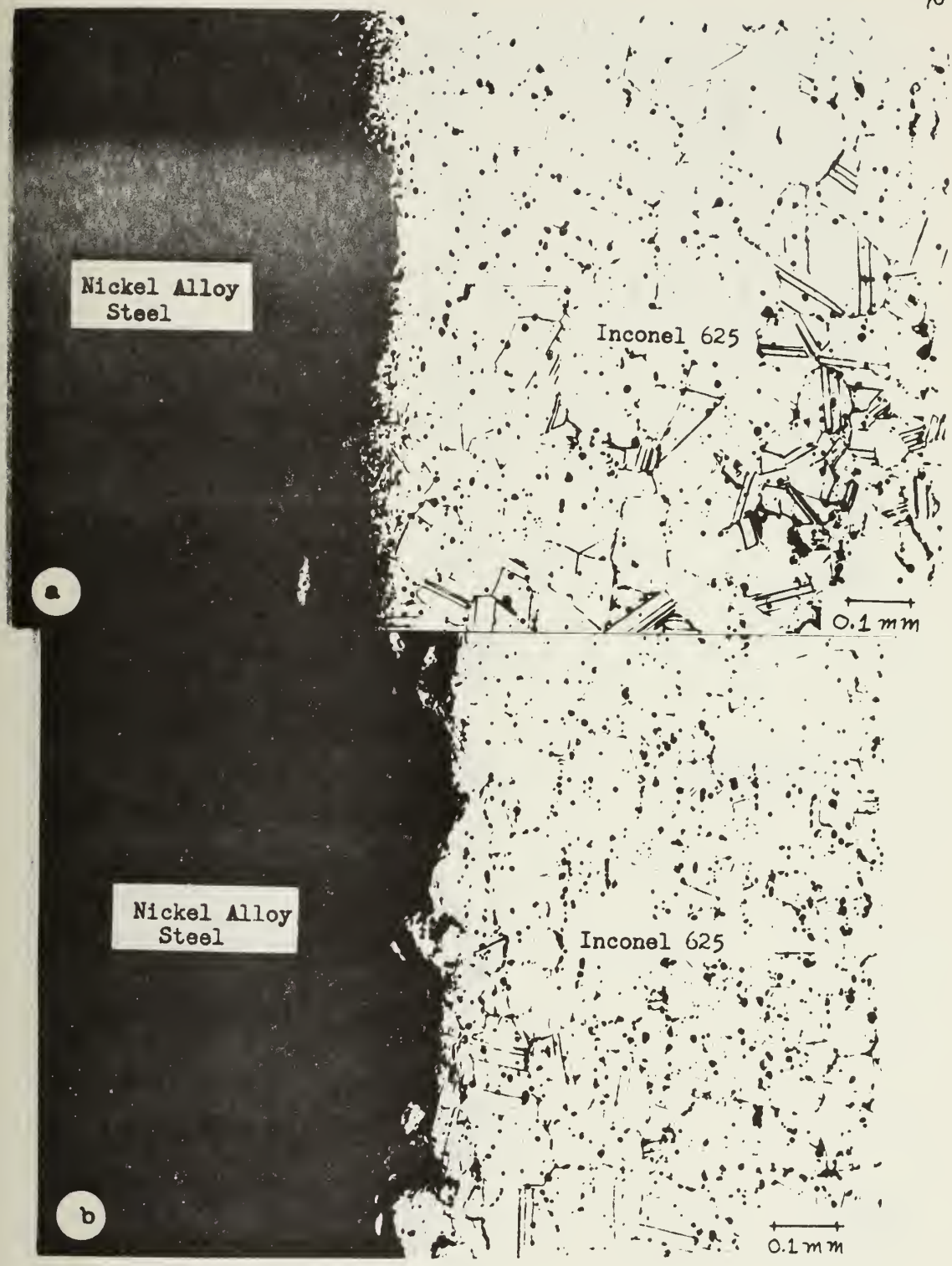

Figure 12 - Short Transverse Interface Section (a) As-Bonded and (b) Stress Relieved

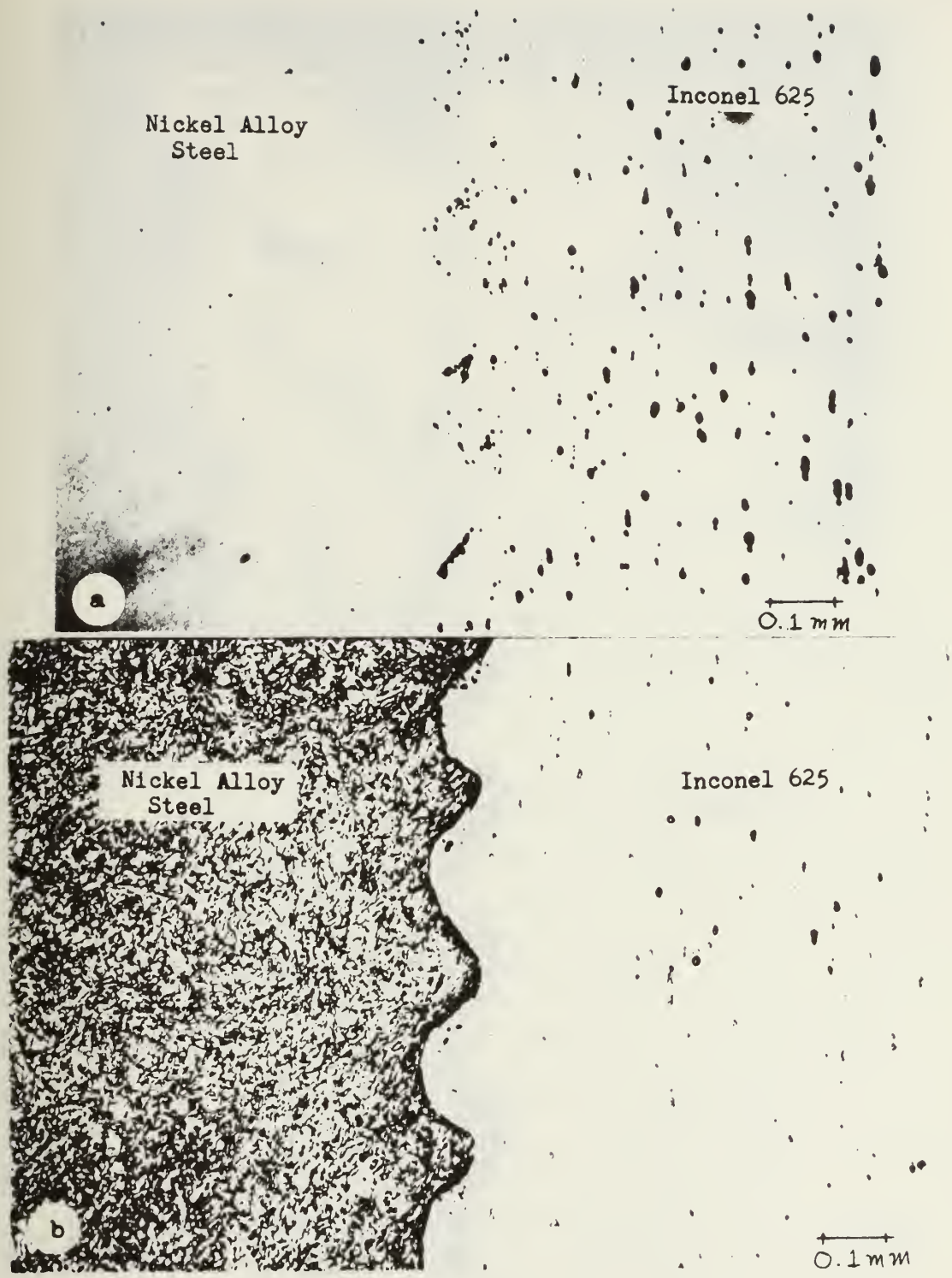

Figure 13 - Longitudinal Interface Section As-Bonded
(a) Unetched and (b) Steel Etched

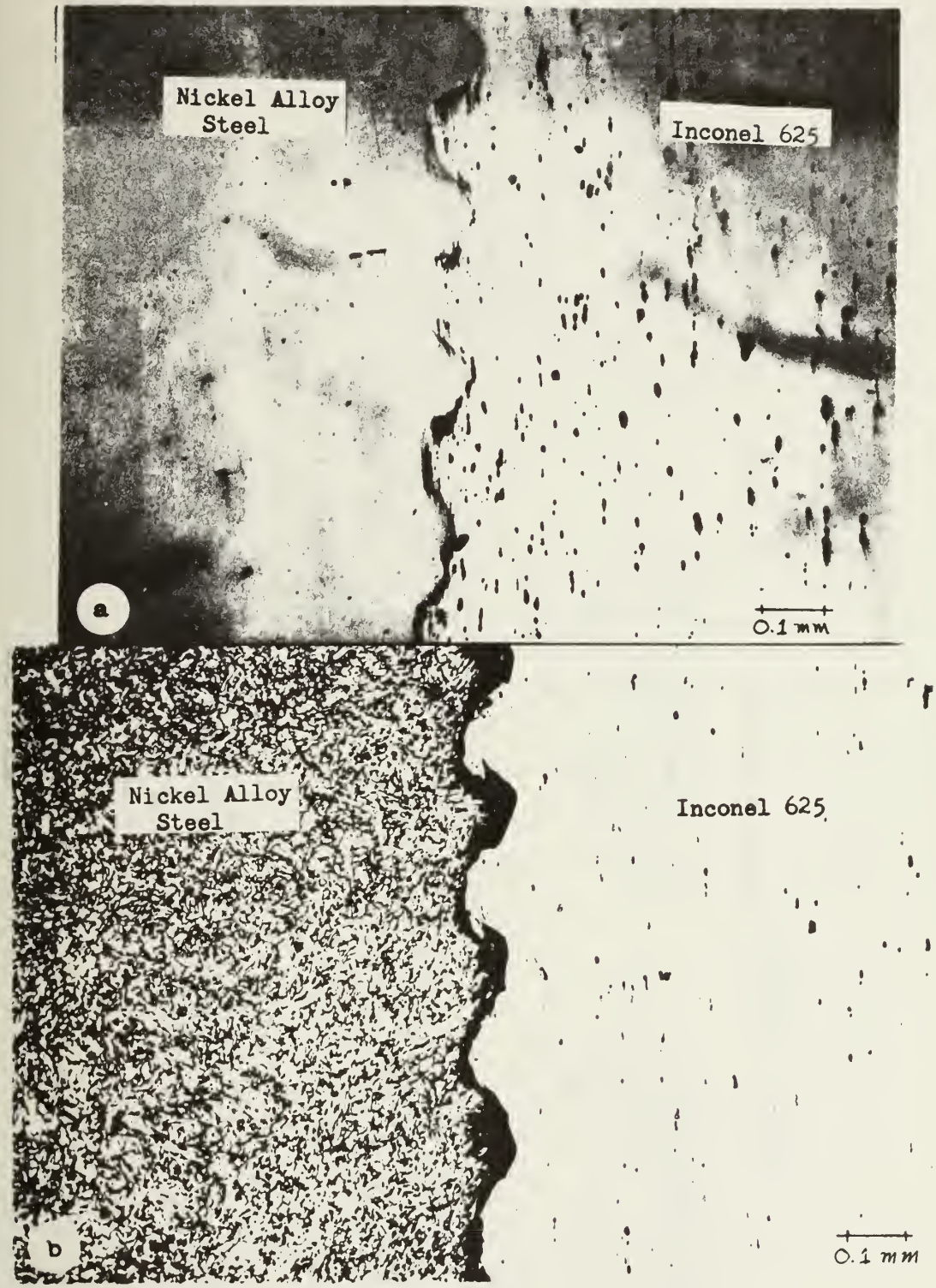

Figure 14 - Longitudinal Interface Section Stress Relieved (a) Unetched and (b) Steel Etched

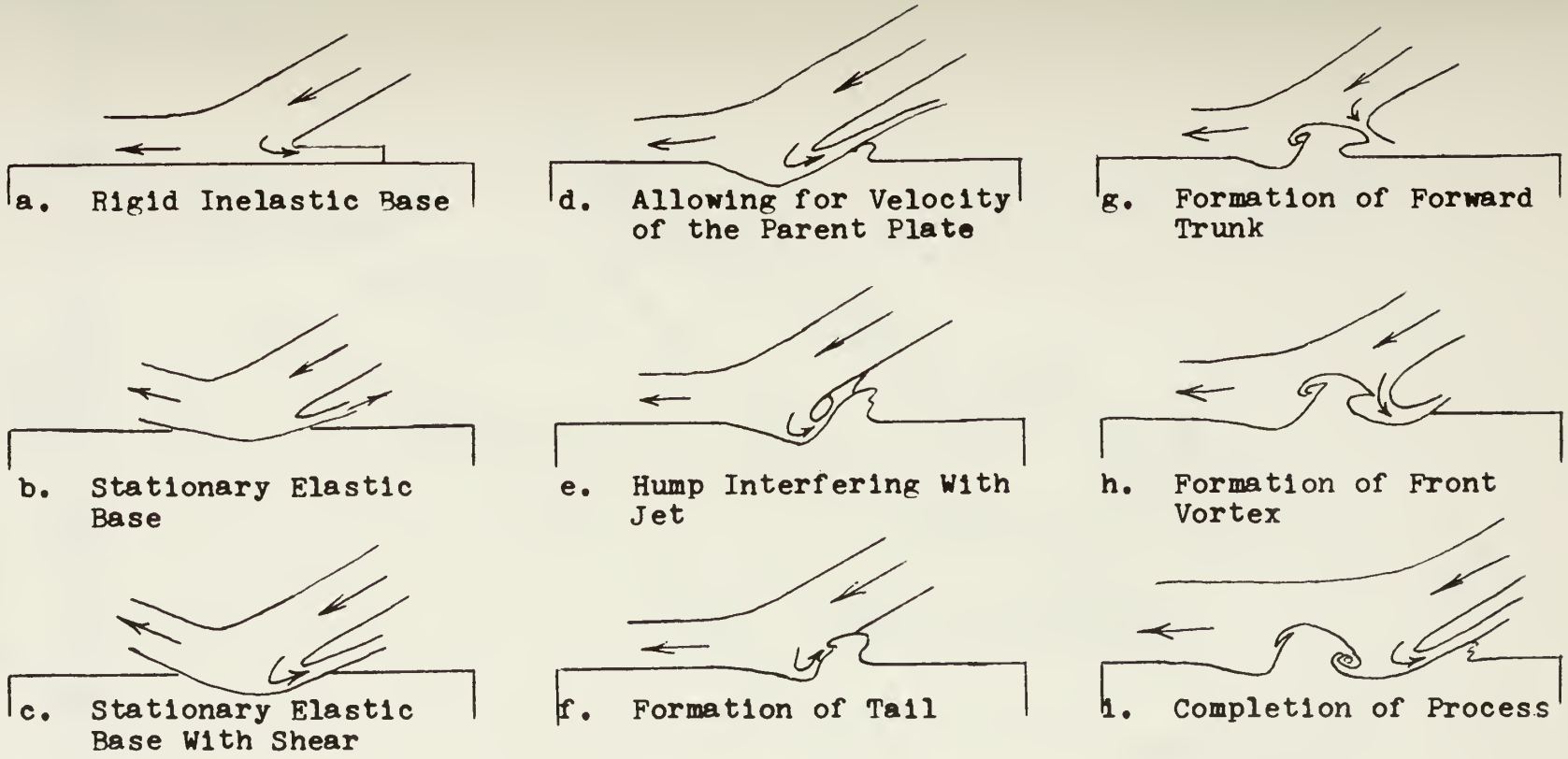

Figure 15 - Schematic Showing the Development of the Wave Formation During the Bonding Process

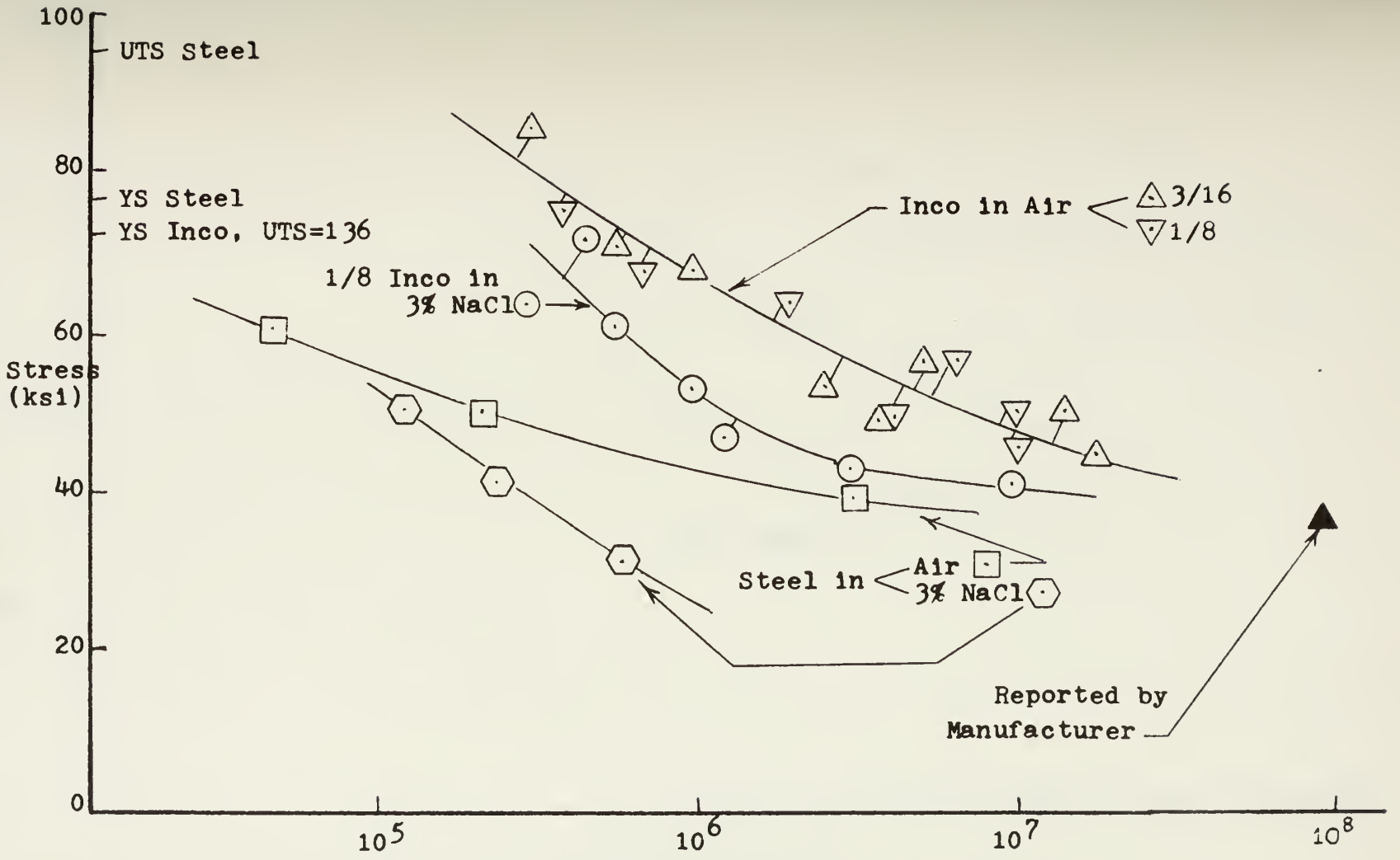

Figure 16 - Fatigue Life Curves for Inconel and Steel

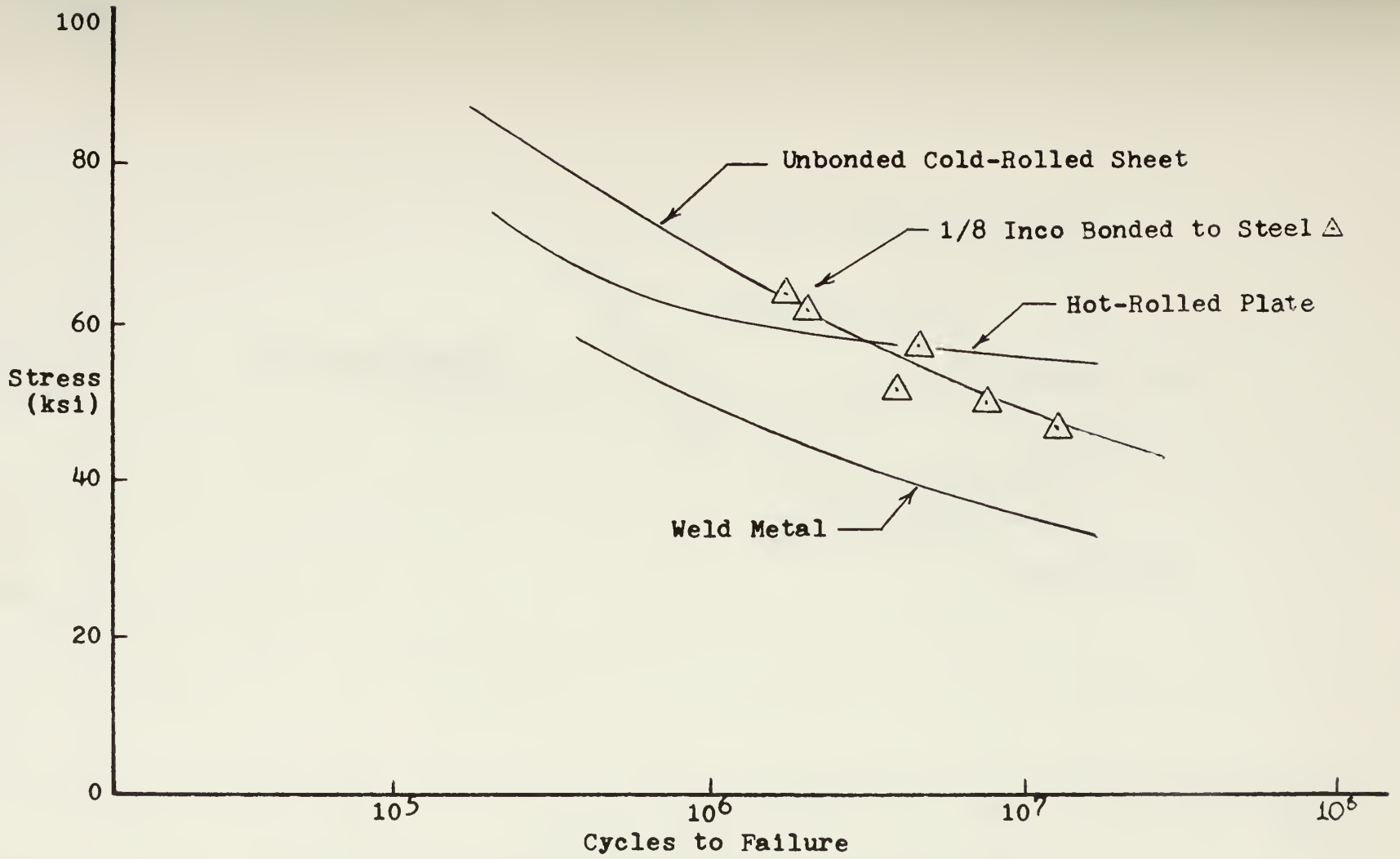

Figure 17 - Points for Bonded Inconel in Air

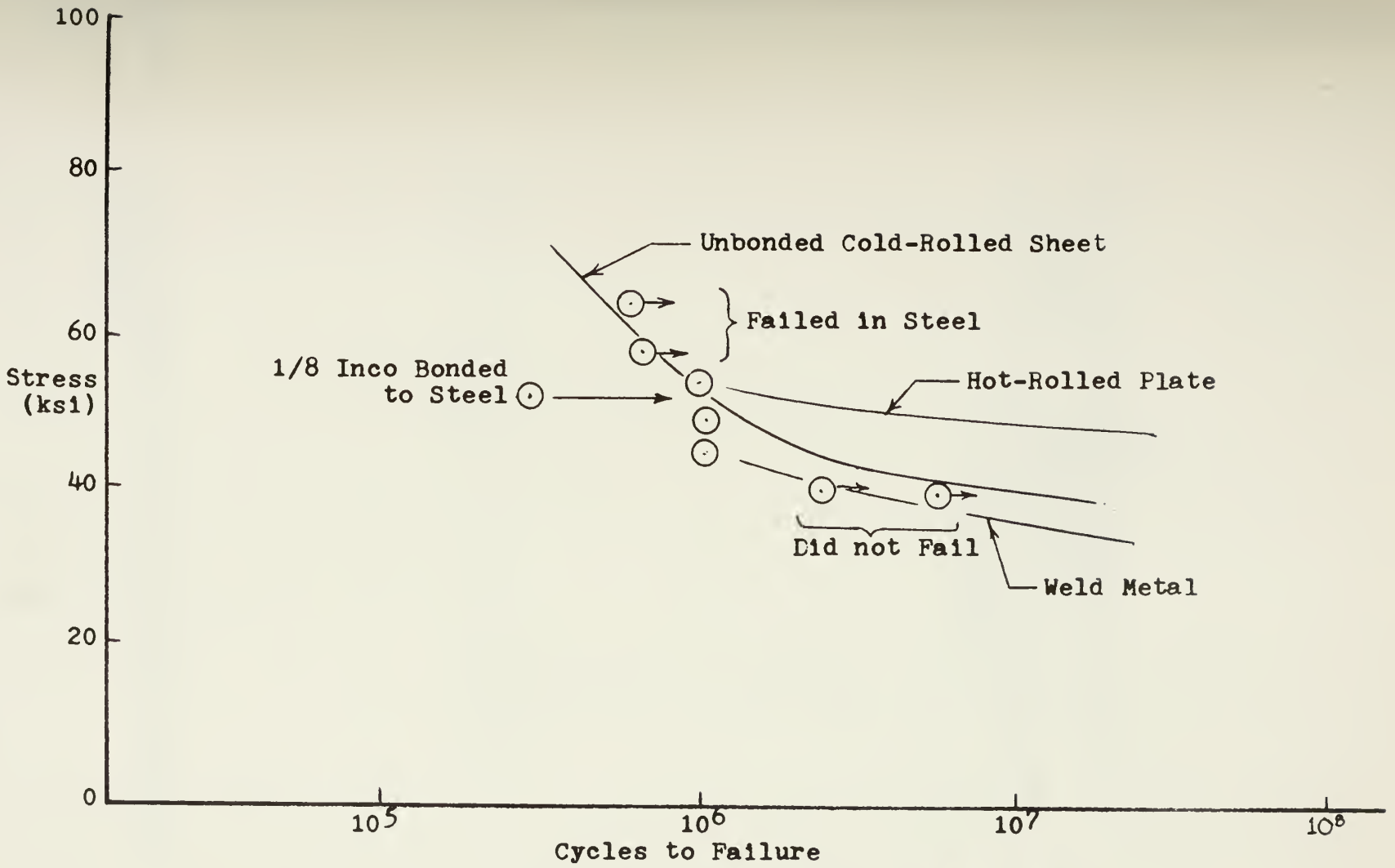

Figure 18 - Points for Bonded Inconel in Salt Water

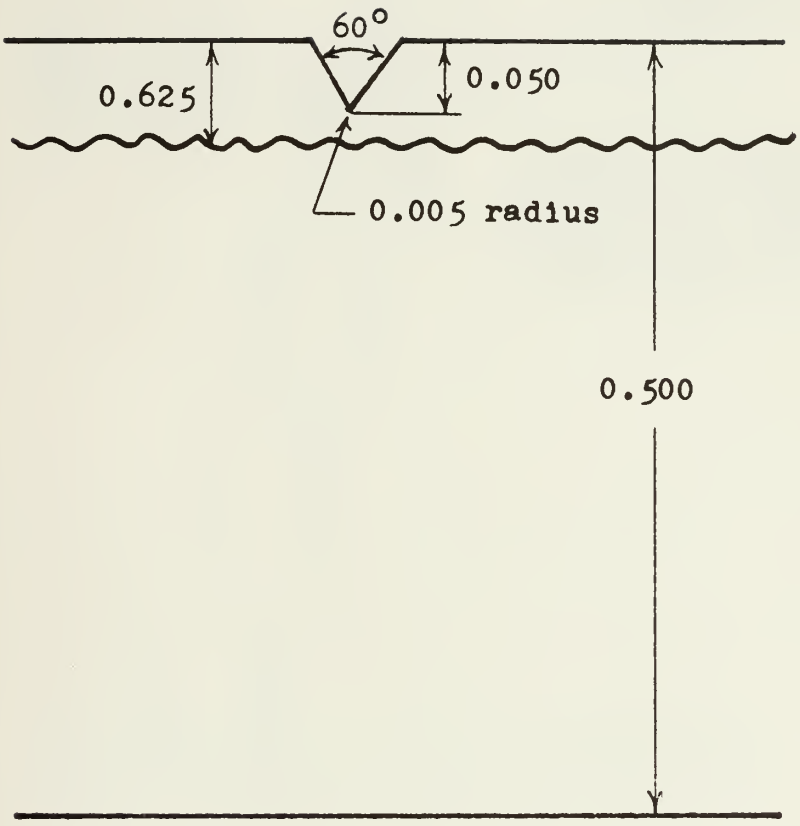

Figure 19 - Notch Geometry for Fatigue Crack Propagation Specimens

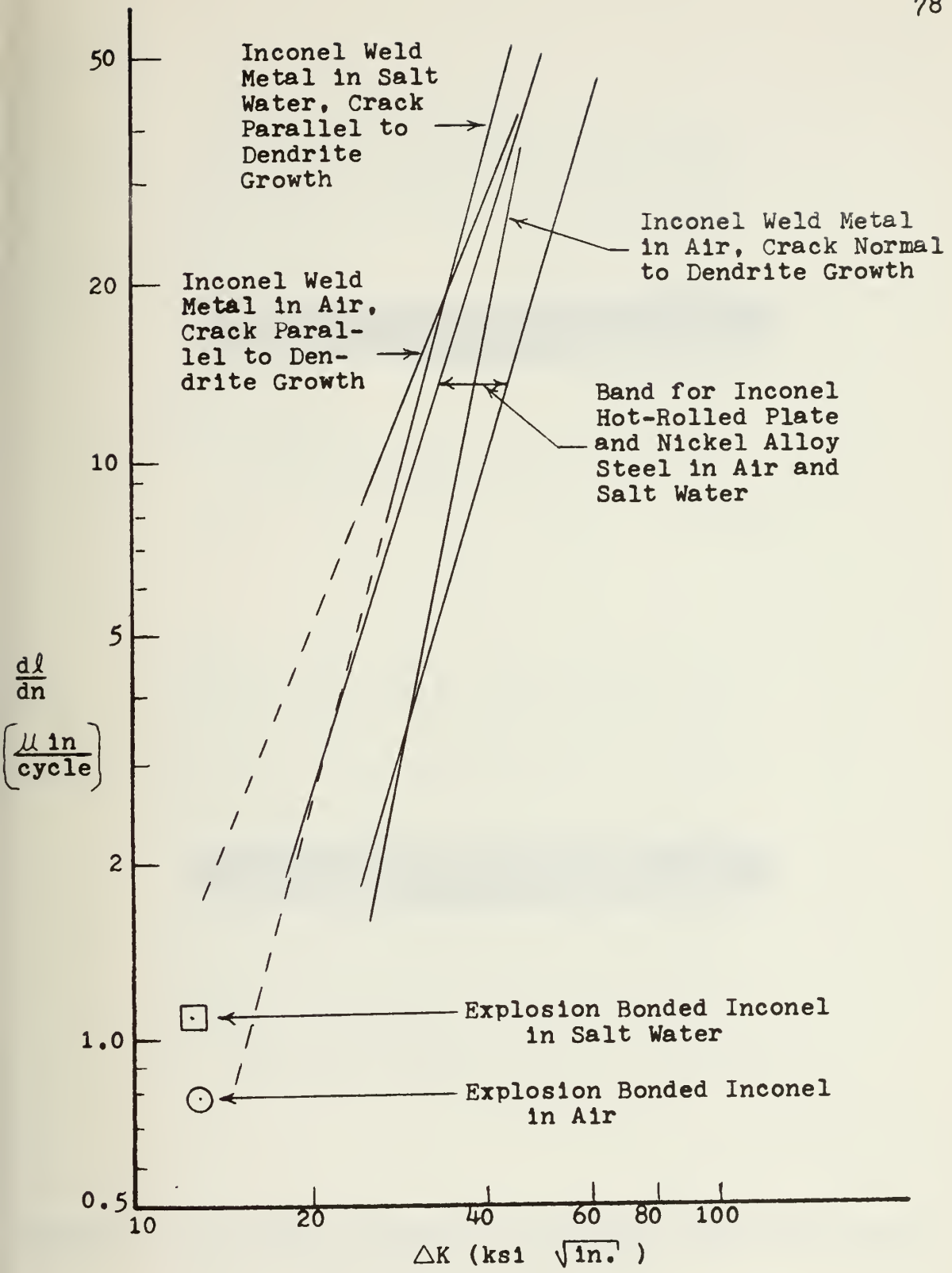

Figure 20 - Comparison of Bonded Crack Growth Rates with the Curves of Long.

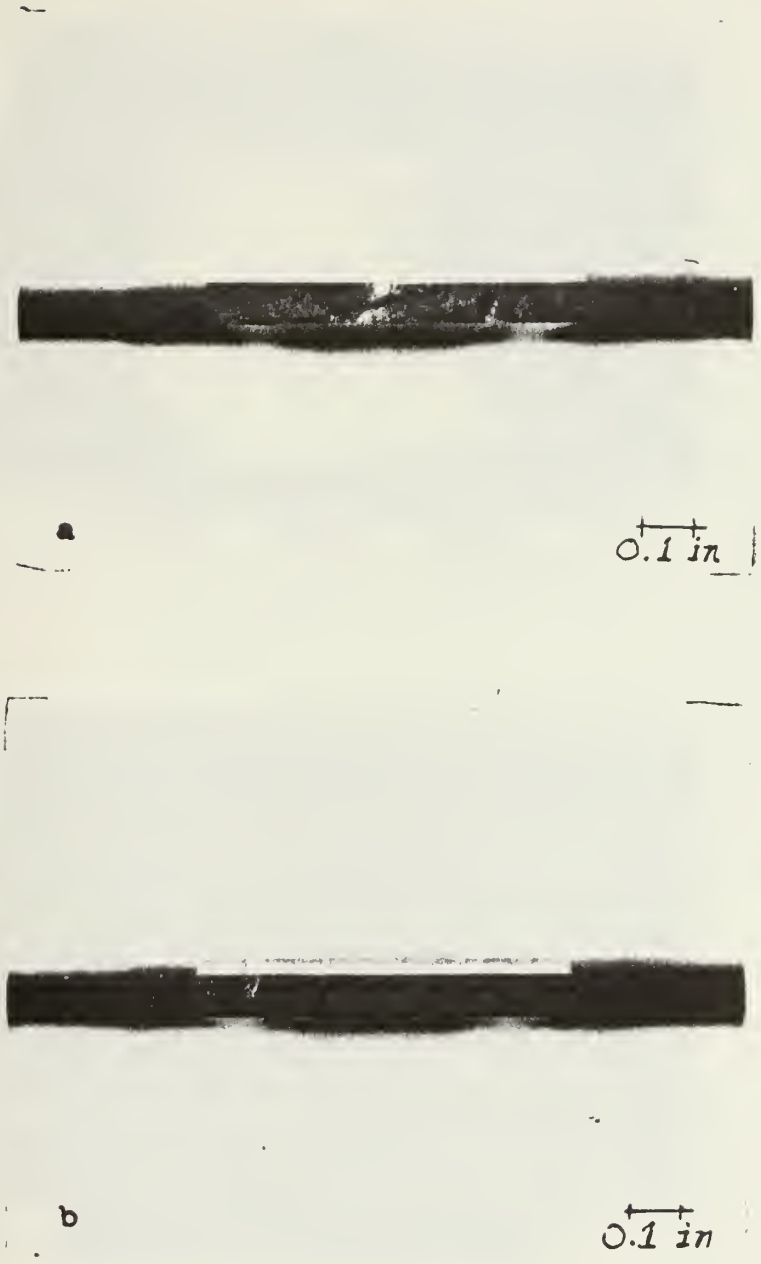

Figure 21 - Fracture Surfaces of Unbonded Specimens Tested in (a) Air and (b) Salt Water.

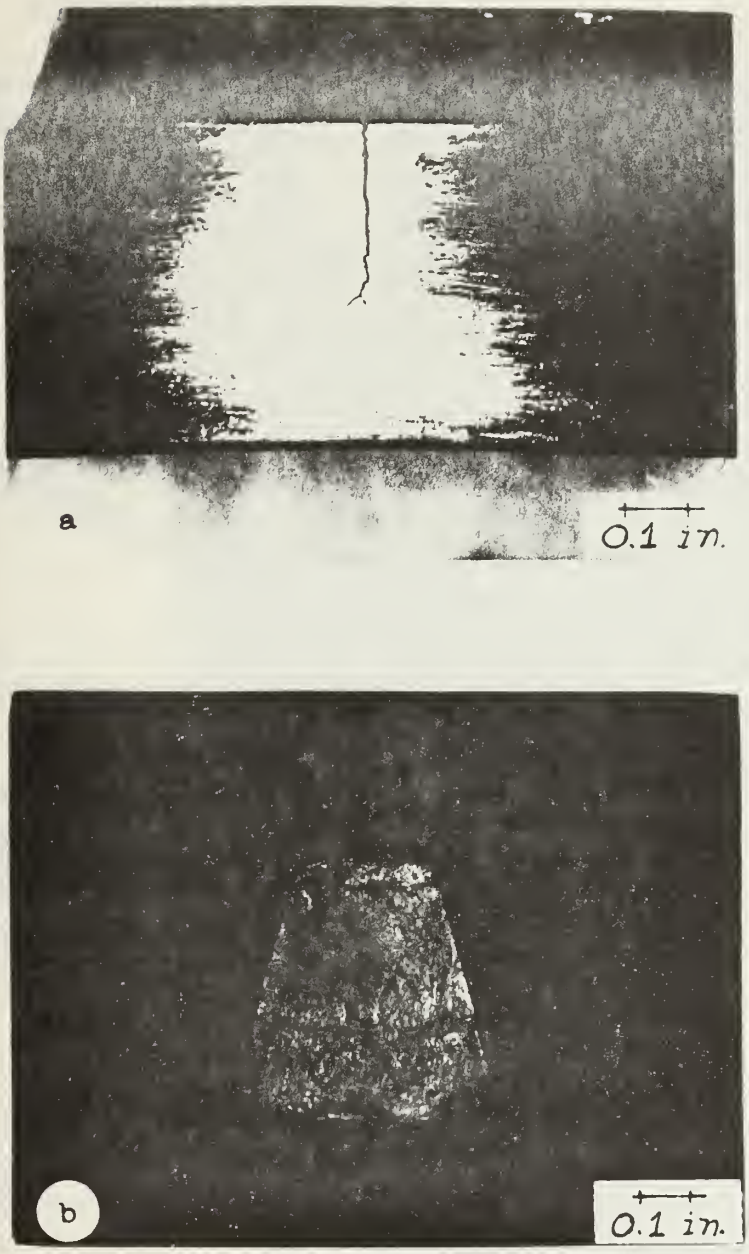

Figure 22 - Bonded Specimen Tested in Air

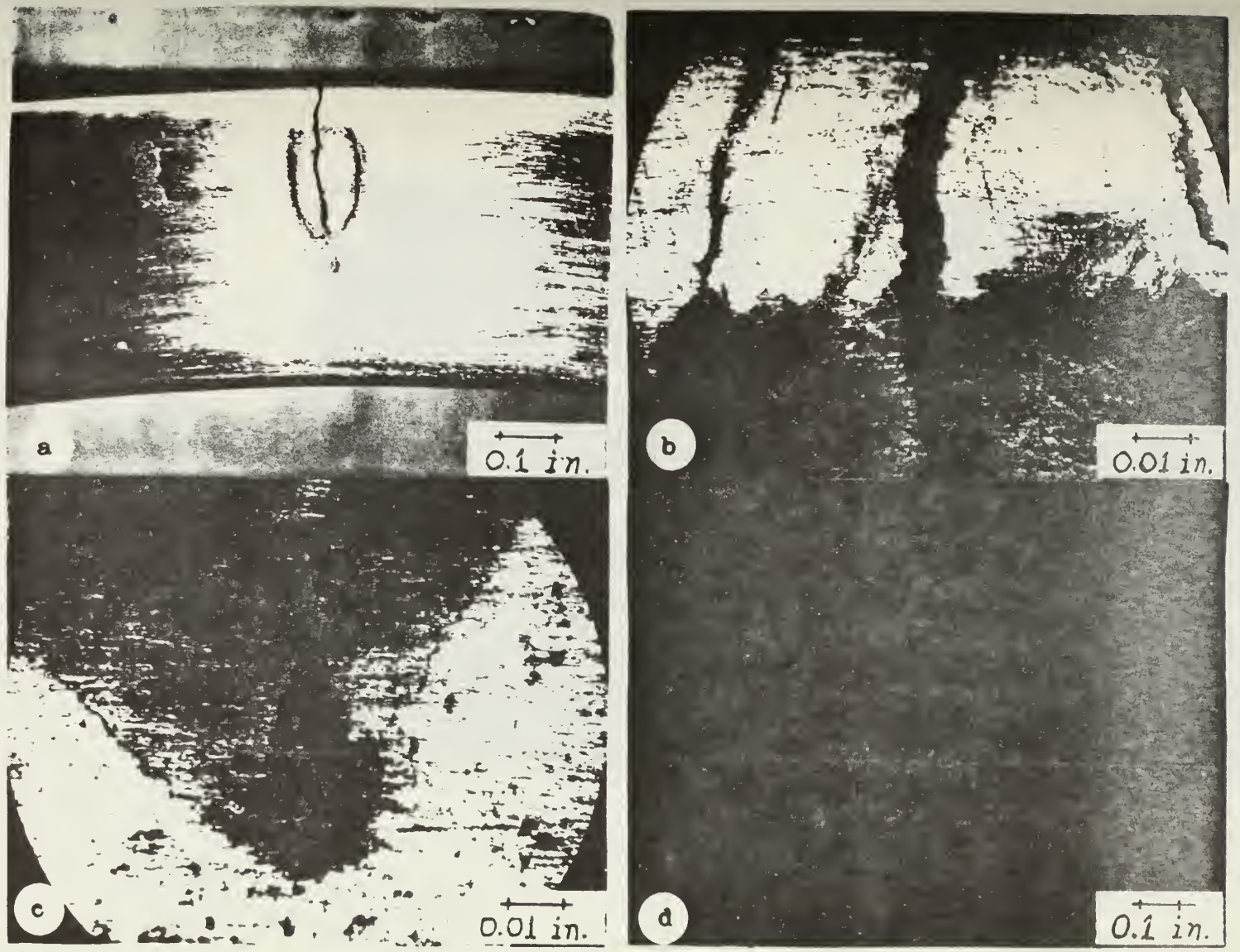

Figure 23 - Bonded Specimen Tested in Salt Water

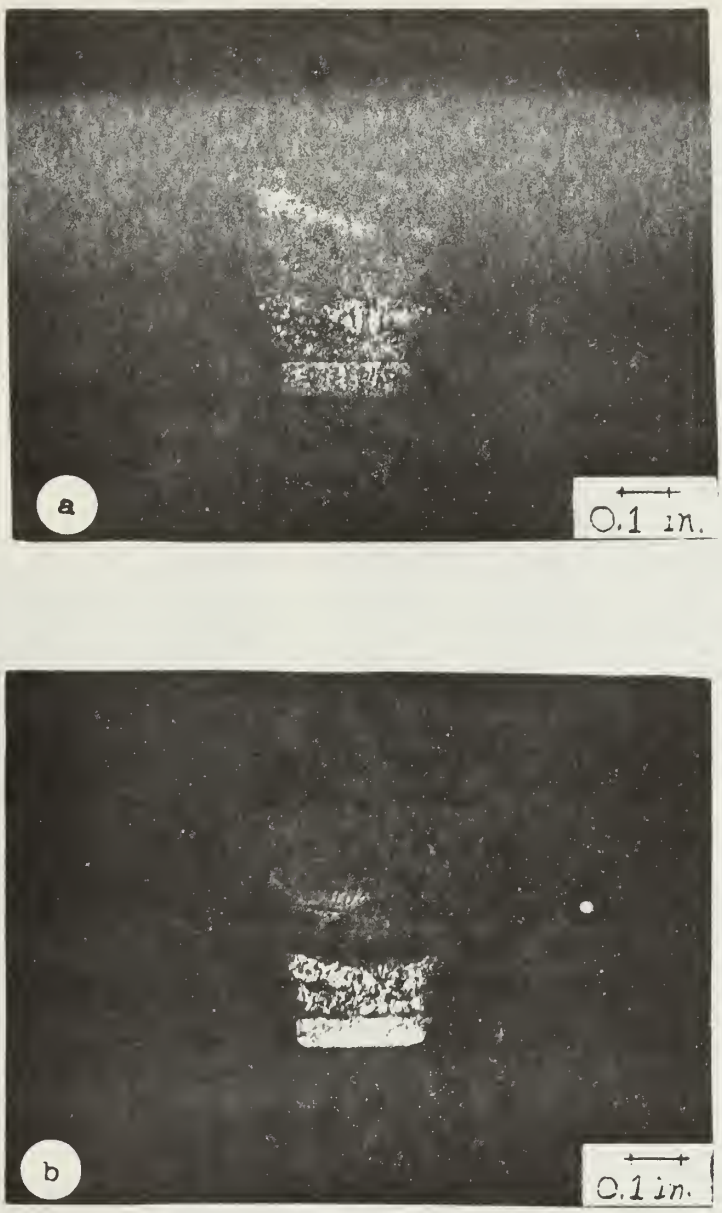

Figure 24 - Fracture Surfaces of Bonded Specimens in Which the Crack Initiated in the Steel Tested in (a) Air and (b) Salt Water

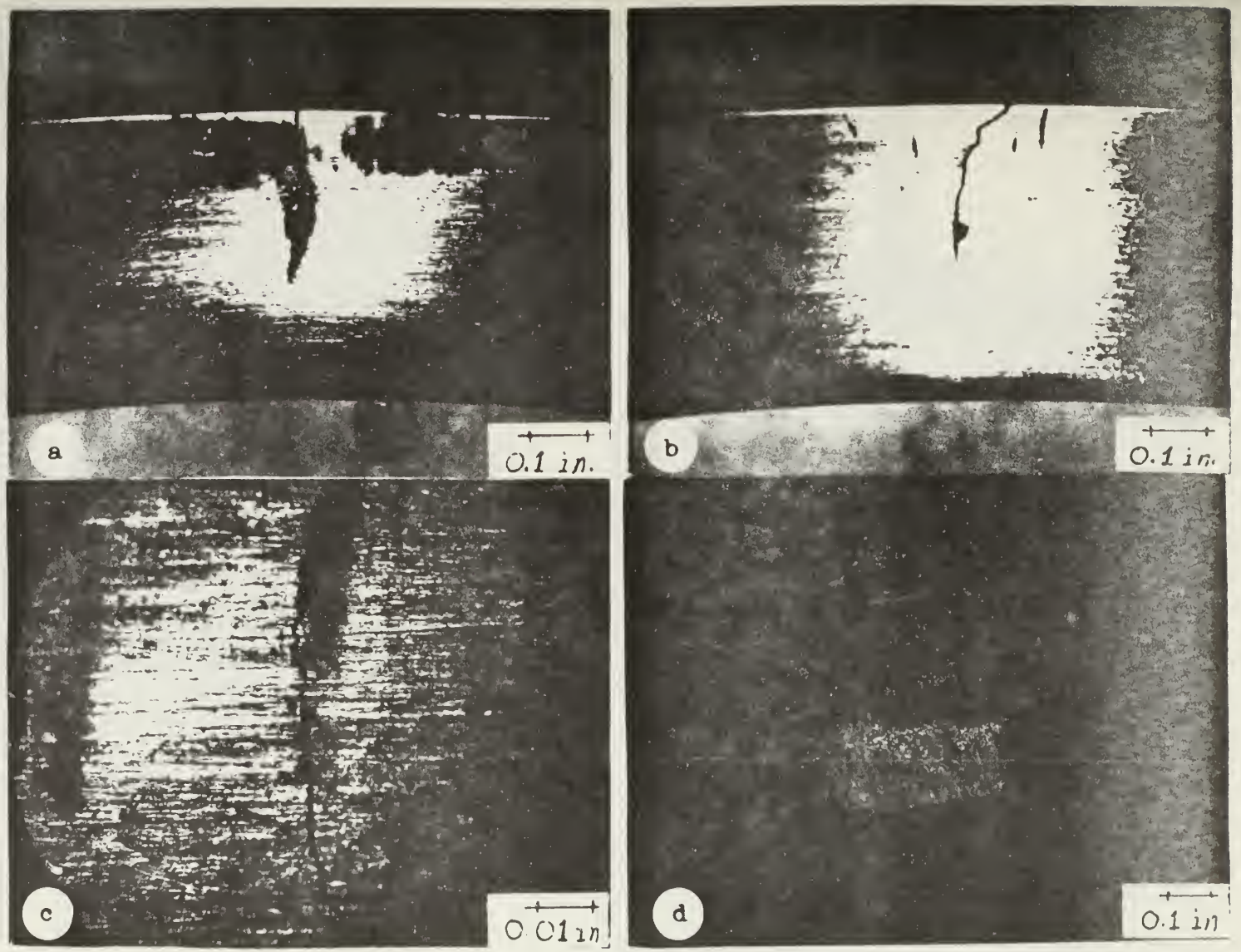

Figure 25 - Bonded Specimen Tested in Salt Water with the Interface Exposed

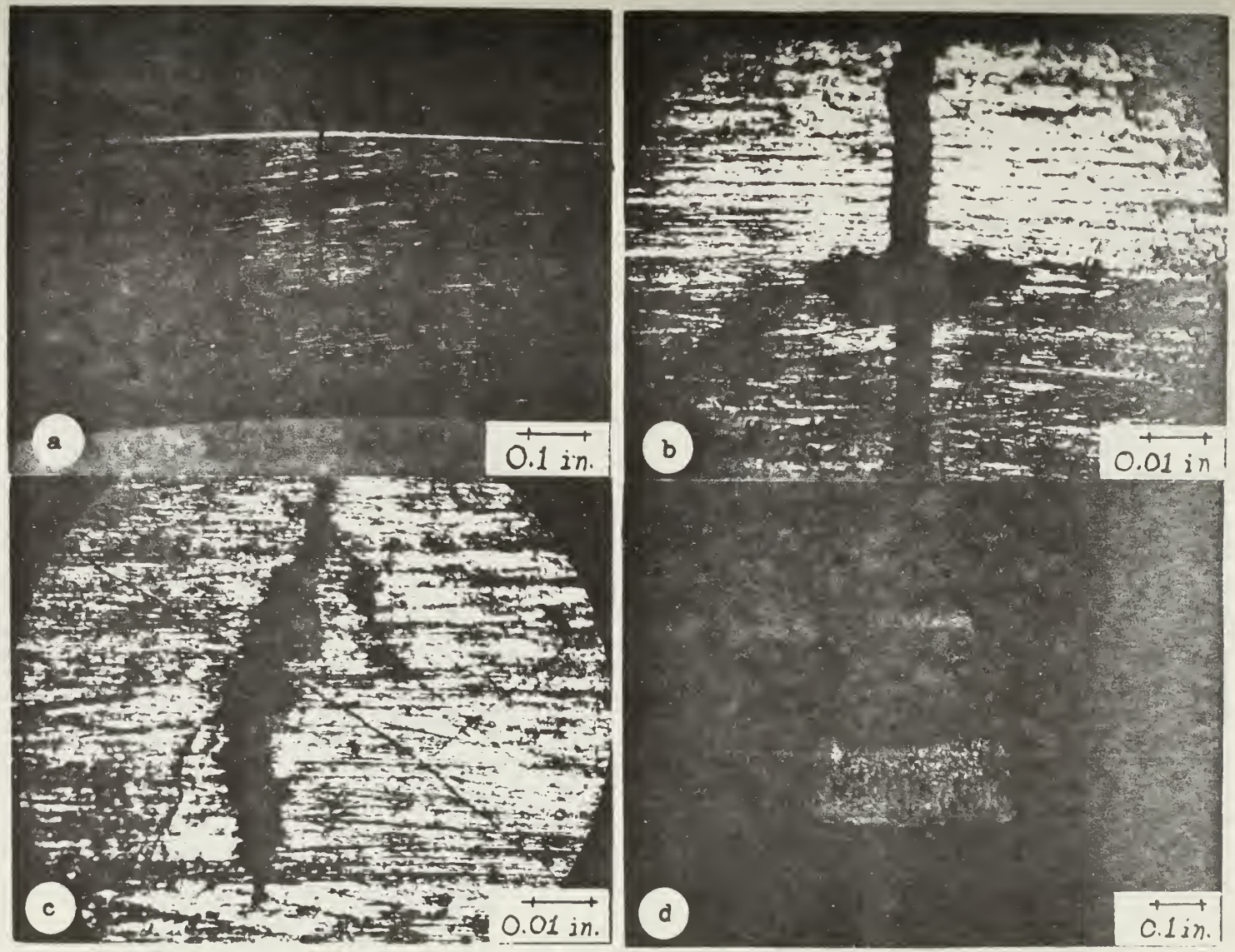

Figure 26 - Bonded Specimen Tested in Salt Water with a Defect in the Coating

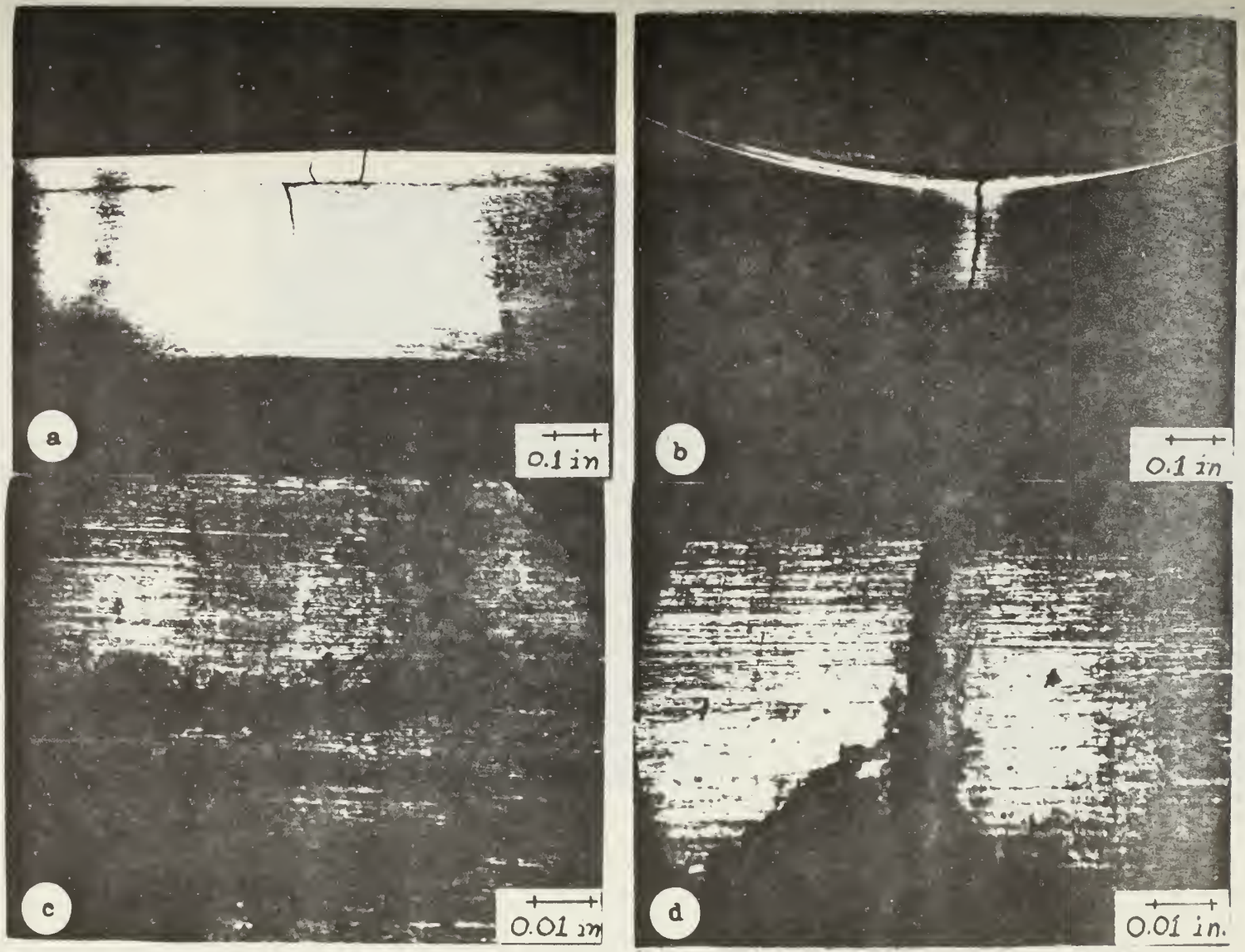

Figure 27 - Specimen Bonded with a Defect Tested in Salt Water

Figure 28 - Fracture Surface of Specimen Bonded with a Defect Tested in Salt Water

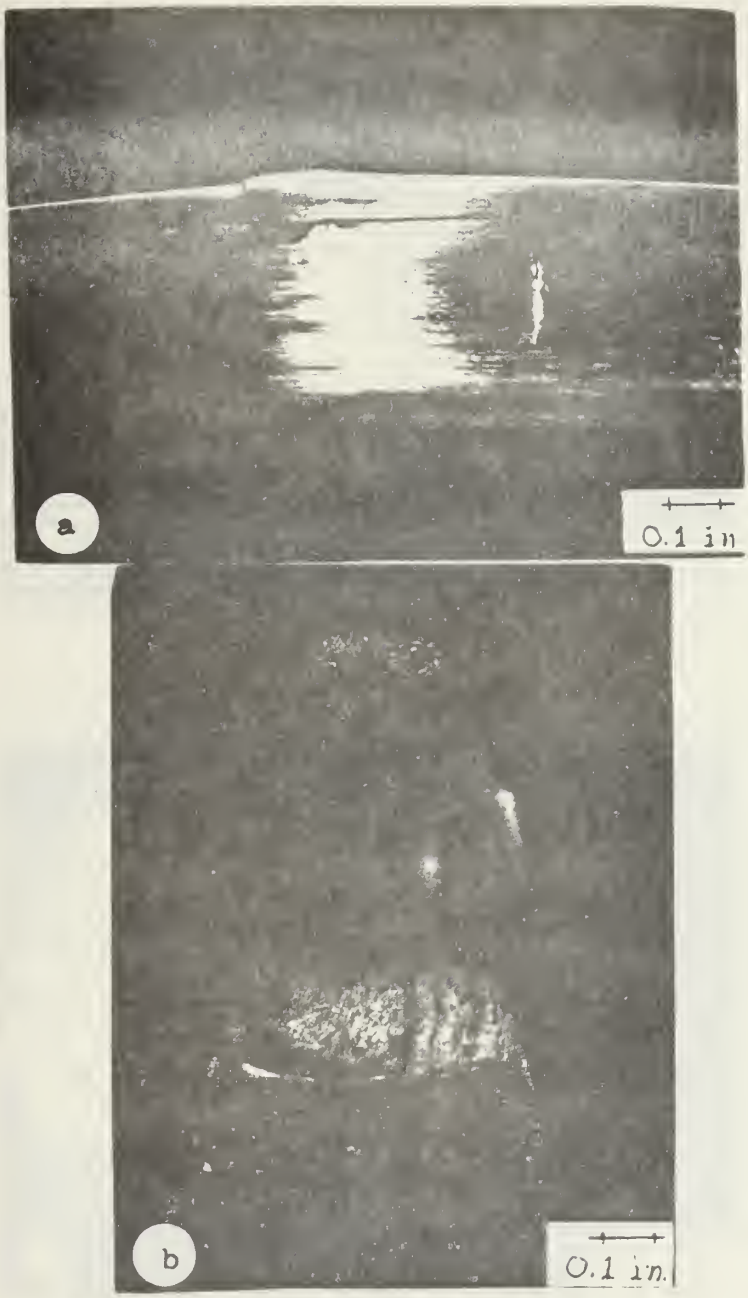

Figure 29 - Specimen Bonded with a Defect Tested in (a) Salt Water and (b) Air

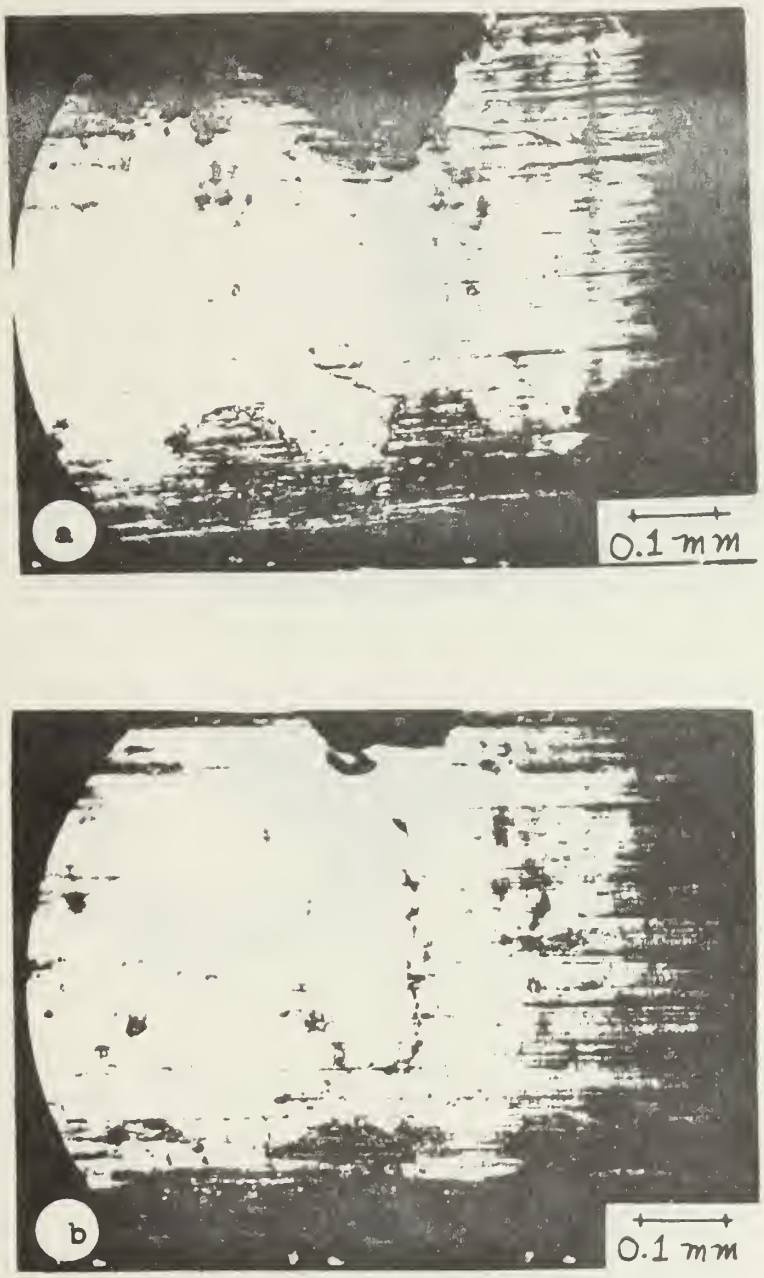

Figure 30 - Crack Propagation Specimen Tested in Air

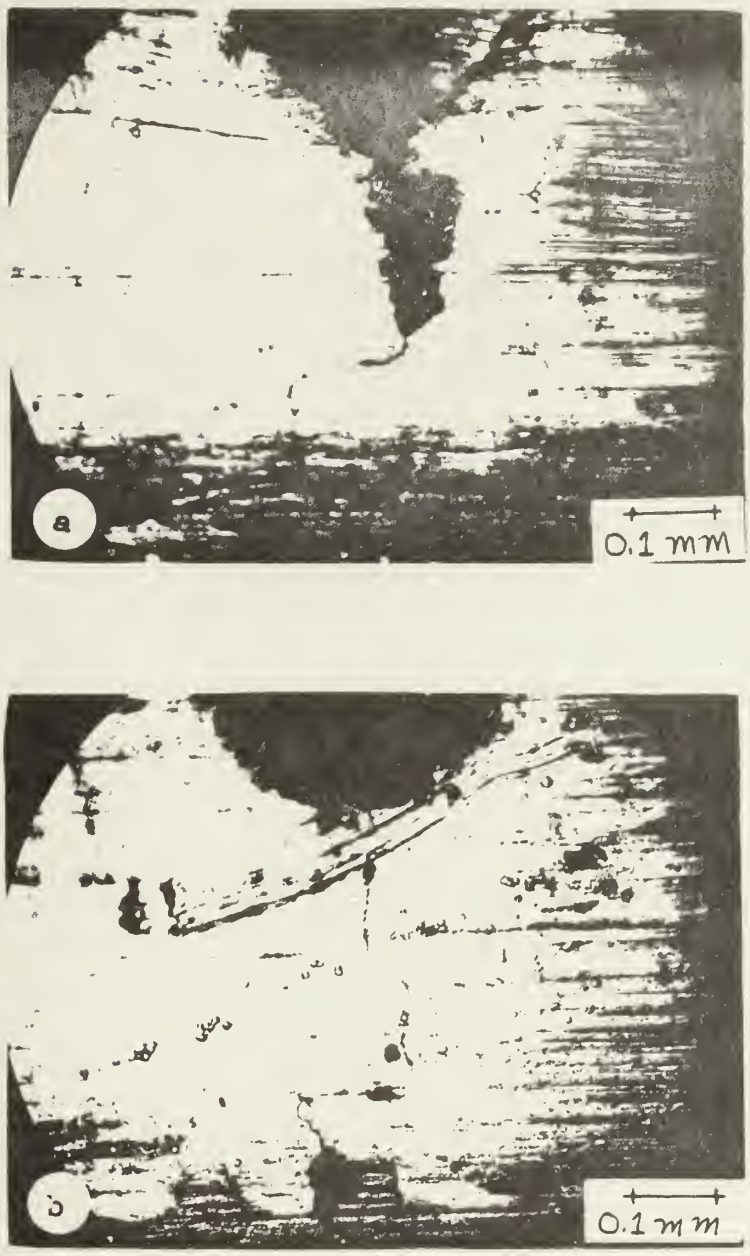

Figure 31 - Crack Propagation Specimen Tested in Salt Water

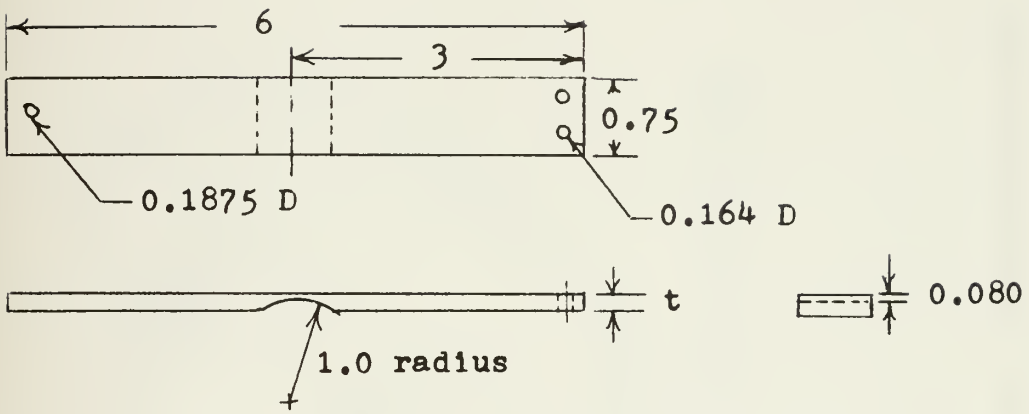

Figure A1 - Specimen Design for Unbonded Inconel

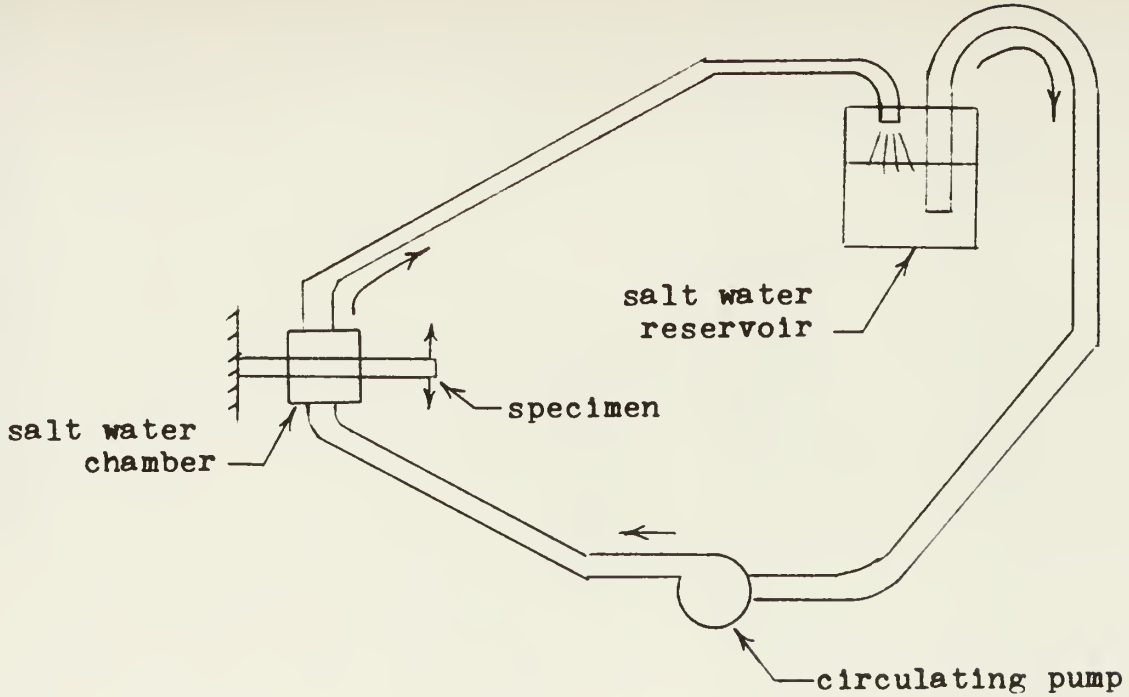

Figure A2 - Schematic of Salt Water Circulating System

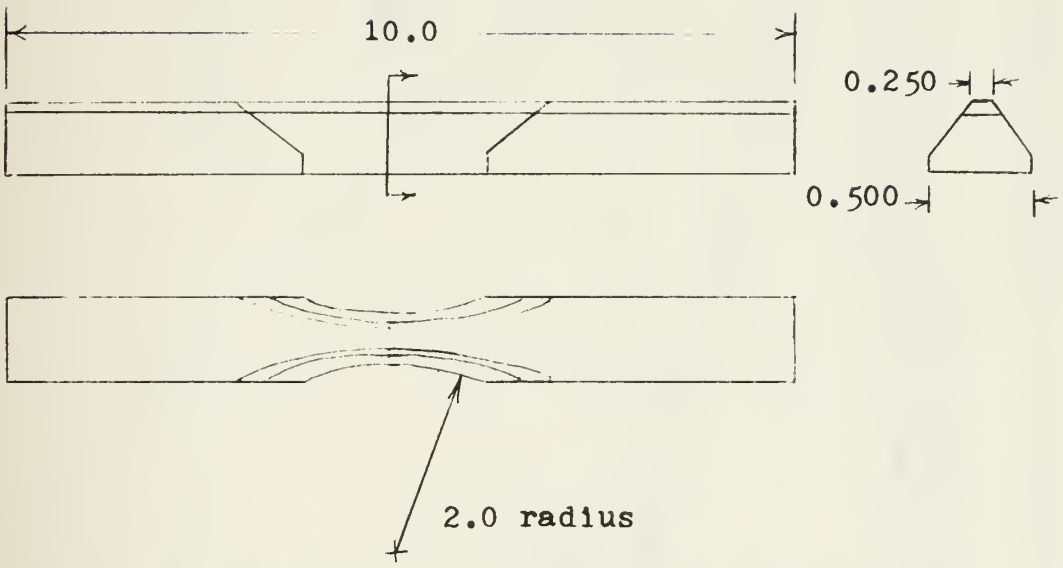

Figure A3 - Bonded Specimen Design

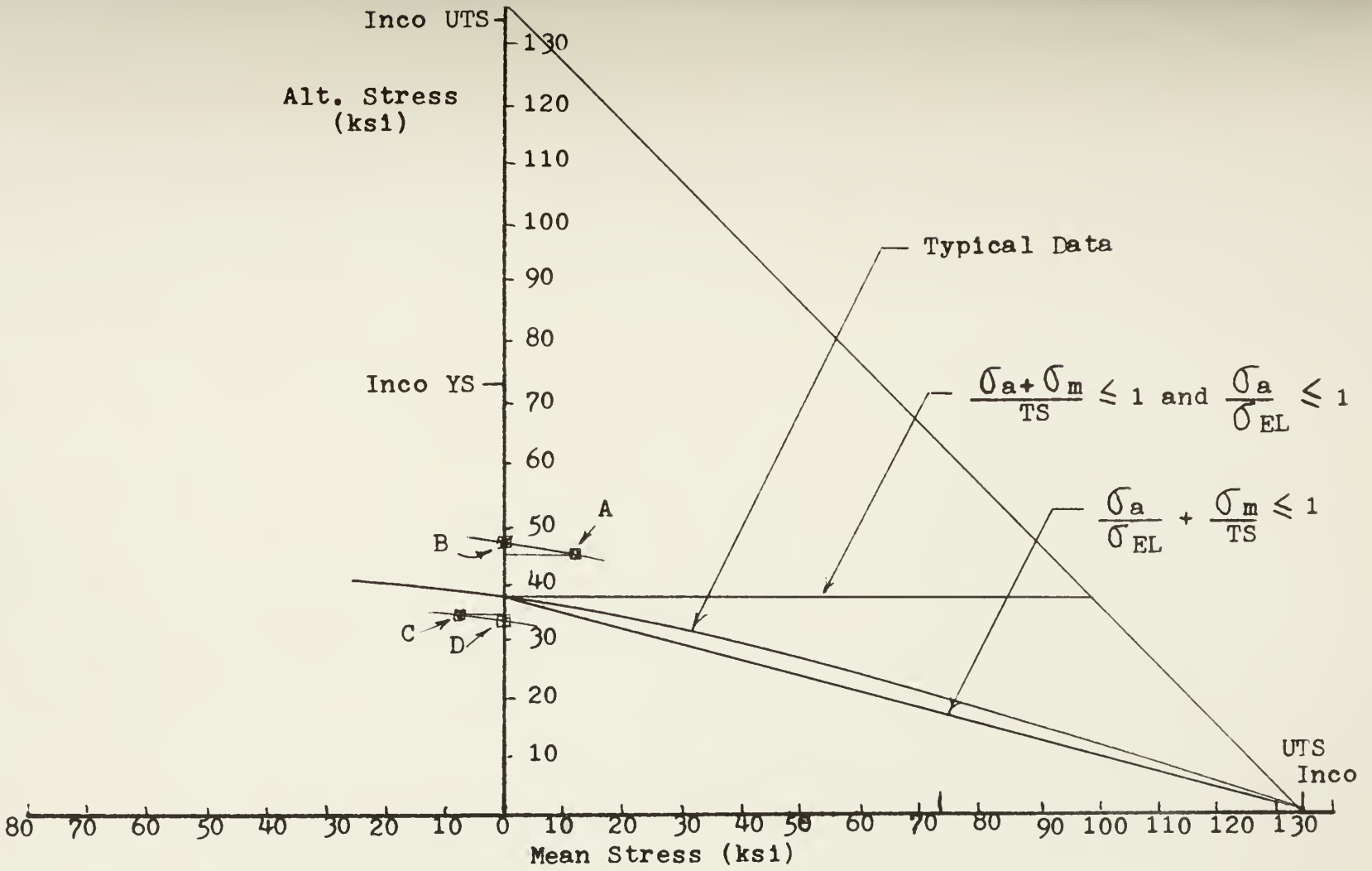

Figure A4 - Combined Stress Pattern for Determining Equivalent Stress

Thesis
S2423 Scalzo
Corrosion fatigue of
Inconel 625 explosion
bonded to nickel alloy
steel.
145798